

Angular Combining of Forecasts of Probability Distributions

James W. Taylor

Saïd Business School, University of Oxford, UK, james.taylor@sbs.ox.ac.uk

Xiaochun Meng

School of Management, University of Bath, UK, xiaochun.meng@bath.edu

When multiple forecasts are available for a probability distribution, forecast combining enables a pragmatic synthesis of the information to extract the wisdom of the crowd. The linear opinion pool has been widely used, whereby the combining is applied to the probabilities of the distributional forecasts. However, it has been argued that this will tend to deliver overdispersed distributions, prompting the combination to be applied, instead, to the quantiles of the distributional forecasts. Results from different applications are mixed, leaving it as an empirical question whether to combine probabilities or quantiles. In this paper, we present an alternative approach. Looking at the distributional forecasts, combining the probabilities can be viewed as vertical combining, with quantile combining seen as horizontal combining. Our proposal is to allow combining to take place on an angle between the extreme cases of vertical and horizontal combining. We term this angular combining. The angle is a parameter that can be optimized using a proper scoring rule. For implementation, we provide a pragmatic numerical approach and a simulation algorithm. Among our theoretical results, we show that, as with vertical and horizontal averaging, angular averaging results in a distribution with mean equal to the average of the means of the distributions that are being combined. We also show that angular averaging produces a distribution with lower variance than vertical averaging, and, under certain assumptions, greater variance than horizontal averaging. We provide empirical results for distributional forecasts of Covid mortality, macroeconomic survey data, and electricity prices.

Key words: probabilistic forecasting; forecast combining; probability distributions; quantiles.

1. Introduction

Predictions of probability distributions convey forecast uncertainty and are of great importance for many applications. For example, forecasts of a distribution's tails are the focus in economic and financial risk management (Brownlees and Souza 2021; Wang and Zitikis 2021); quantile forecasts are needed to enable optimal decision making in newsvendor contexts (Arrow et al. 1951); efficient

call center workforce planning requires forecasts of the distribution and quantiles of call arrival rates (Ye et al. 2019); and, in epidemic modeling, distributional forecasts provide situational awareness, sometimes in the form of interval forecasts, to support health policy decisions (Bracher et al. 2021).

When forecasts are available from multiple experts or methods, combining is often used as a convenient way to capture the wisdom of the crowd through the synthesis of the different sources of forecast information. Winkler et al. (2019) provide a review of the growing literature on approaches used to combine probabilistic forecasts. They comment that averaging has the appeal, not only of simplicity, but also robustness and competitive empirical performance. However, once a reasonable history of past accuracy becomes available, weighted combinations can be more accurate (Aastveit et al. 2019). When a reasonably large number of distributional forecasts are available, the combining method could be chosen as the median (see Hora et al. 2013) or an approach based on trimmed means. Quite apart from enabling robustness to outliers, trimming the outermost or innermost distributions from a set of distributional forecasts can be used to control the dispersion of the resulting combined distributional forecast (Jose et al. 2014; Grushka-Cockayne et al. 2017a).

To combine forecasts of continuous distributions, Lichtendahl et al. (2013) consider whether it is better to average probabilities or quantiles. They note that, although averaging probabilities is more common, it is a concern that, for a set of calibrated distributional forecasts, averaging probabilities will deliver a forecast that is not calibrated and is too wide (see also Hora 2004; Gneiting and Ranjan 2013). Lichtendahl et al. (2013) point out that averaging quantiles has some appealing theoretical properties, most notably that it leads to a distributional forecast that has lower variance than averaging probabilities. However, individual distributional forecasts can be underdispersed, in which case averaging quantiles can produce an underdispersed distributional forecast. Indeed, drawing on empirical results, Cooke et al. (2021) advise against averaging quantiles. Given conflicting recommendations, a pragmatic approach is to consider it an empirical question as to whether it is better, for a particular application, to combine probabilities or quantiles. Ideally, one should let the data decide.

In this paper, for continuous distributions, we propose an alternative averaging approach that lies between averaging probabilities and averaging quantiles. With averaging probabilities viewed as

averaging vertically, and averaging quantiles viewed as averaging horizontally, our alternative is to average at an angle between these two extremes. The angle is a parameter that can be optimized using past data and a proper scoring rule. With the angle suitably chosen, the new method can be viewed as finding the right balance between vertical and horizontal averaging. This *angular averaging* is a practical proposal that extends and encompasses vertical and horizontal averaging.

Our theoretical results build on several results provided by Lichtendahl et al. (2013) for vertical and horizontal averaging. We show that, like vertical and horizontal averaging, angular averaging delivers a distribution for which the mean is the average of the means of the distributions in the combination. We also show that angular averaging produces a distribution with lower variance than vertical averaging, and, under certain assumptions, greater variance than horizontal averaging. Furthermore, under these assumptions, the variance is a monotonic function of the angle. Drawing on our results for the mean and variance of angular averaging, we address when to use this combining method by describing a situation where it should be preferred to horizontal and vertical averaging. For a popular scoring rule, we find that the score for angular averaging is no worse than the average score of the distributional forecasts in the combination. Other forms of angular combining can also be considered, such as performance-based weighted averaging. Hora et al. (2013) show that median aggregation results in the same distribution regardless of whether the median is obtained vertically or horizontally. We find that the same distribution is produced when the median is obtained at an angle.

Section 2 provides background for our proposal by discussing vertical and horizontal combining. Section 3 presents angular averaging followed by consideration of other forms of angular combining. Section 4 presents theoretical results for angular combining. Section 5 provides our main empirical study, which evaluates the new proposals using forecasts for weekly Covid mortality at the national and state level in the U.S. Section 6 presents additional empirical studies, involving forecasts of macroeconomic variables and electricity prices. Section 7 provides a summary and concluding comments.

2. Vertical and Horizontal Combining of Distributional Forecasts

In this section, we describe the contrasting approaches of vertical and horizontal combining. We go into some depth, as we feel this is important for the presentation of our new proposals in Section 3. For simplicity, we focus mainly on averaging, and then briefly consider other combining approaches.

2.1. Vertical and Horizontal Averaging

Lichtendahl et al. (2013) illustrate the differences that can result from vertical and horizontal averaging using figures showing the averaging of two Gaussian cumulative distribution functions (CDFs) with different means but identical variances. We repeat similar figures here to assist the explanation of our proposals later in the paper. Figure 1(a) shows the CDF that results from the vertical averaging of two Gaussian CDFs that have means of -0.15 and 0.15 , and standard deviations of 0.1 . Figure 1(b) presents the corresponding probability density functions (PDFs). Figure 2(a) shows the CDF resulting from horizontal averaging of the two Gaussian CDFs. The corresponding PDFs are presented in Figure 2(b). Comparing Figures 1 and 2, we see that noticeably different distributions can result from the two forms of averaging. Figure 1 shows that a bimodal CDF has resulted from the vertical averaging. By contrast, Figure 2 illustrates the result that if the individual distributions are from the same location scale family, such as Gaussian, horizontal averaging leads to a distribution from the same family (Thomas and Ross 1980).

Figure 1 Vertical averaging (in black) of two Gaussian CDFs (in grey) in (a), and corresponding PDFs in (b).

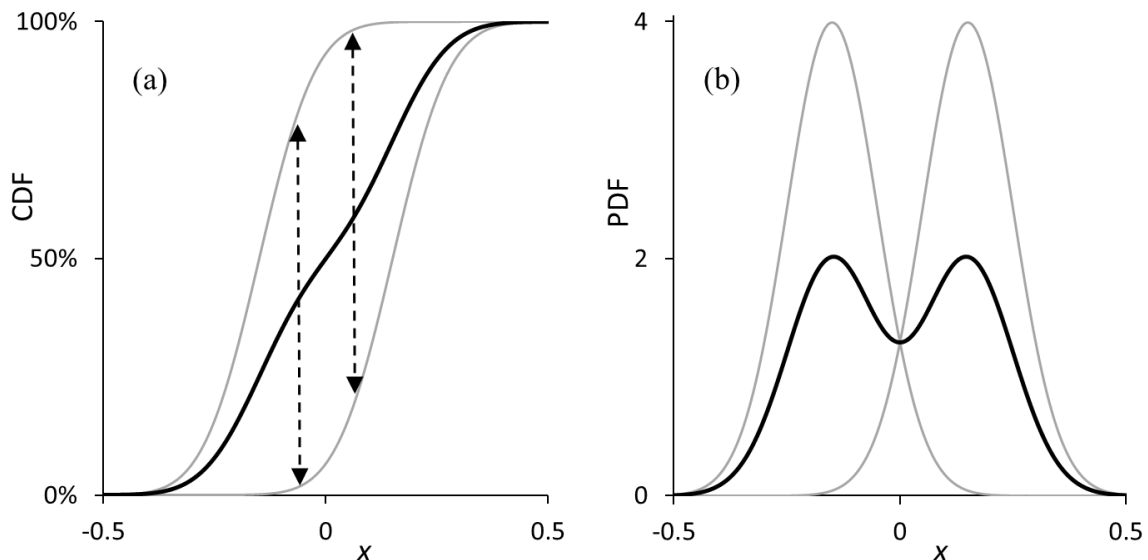
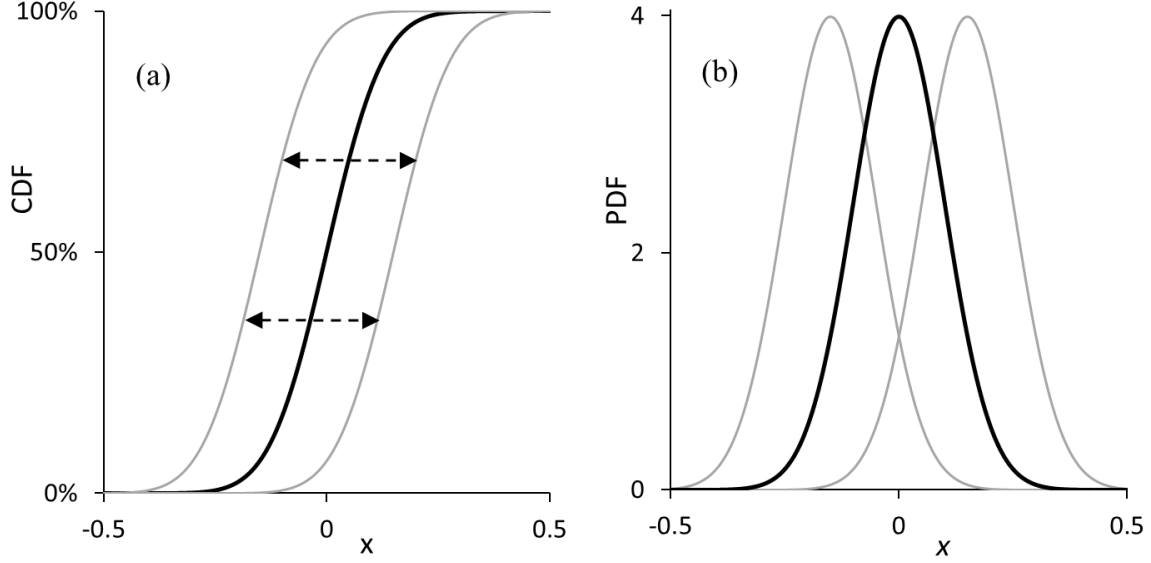


Figure 2 Horizontal averaging (in black) of two Gaussian CDFs (in grey) in (a), and corresponding PDFs in (b).



We note that horizontal combining cannot be used if part of an individual CDF forecast is horizontal, because, for the corresponding value on the y -axis, there would be a set of values of the CDF, and so it would not be clear what CDF value to include in the combination. Therefore, in our discussions of horizontal and vertical combining, we assume each CDF forecast is strictly monotonic.

In this paper, we consider the forecasting of continuous random variables. If we write the CDF and PDF of an individual forecast distribution as F_i and f_i , respectively, the following provides the CDF F_V and PDF f_V of the vertical average of k individual forecast distributions,

$$F_V(x) = \frac{1}{k} \sum_{i=1}^k F_i(x) \quad \text{and} \quad f_V(x) = \frac{1}{k} \sum_{i=1}^k f_i(x). \quad (1)$$

The PDF f_V can be formally derived by differentiating the CDF with respect to (w.r.t.) x .

Given that horizontal averaging involves averaging quantiles, and the α quantile of an individual forecast distribution is $F_i^{-1}(\alpha)$, the first of the following two equations provides an expression in terms of the CDF F_H resulting from horizontal averaging,

$$F_H^{-1}(\alpha) = \frac{1}{k} \sum_{i=1}^k F_i^{-1}(\alpha) \quad \text{and} \quad f_H(F_H^{-1}(\alpha)) = \frac{1}{\frac{1}{k} \sum_{i=1}^k 1/f_i(F_i^{-1}(\alpha))}. \quad (2)$$

Bamber et al. (2016) show that differentiating w.r.t. α each side of the first equation in (2) gives the second equation, which provides an expression for the PDF f_H produced by horizontal averaging.

2.2. Is it better to Average Vertically or Horizontally?

Figures 1 and 2 illustrate the point, shown theoretically by Lichtendahl et al. (2013), that vertical averaging produces a CDF with greater variance than horizontal averaging. They suggest that the CDF forecast produced by vertical averaging will often be too wide, prompting them to propose horizontal averaging as an alternative. Using CDF forecasts from surveys of professional macroeconomic forecasters, they provide empirical results supporting the use of horizontal averaging.

With other applications, it is not clear whether it is preferable to combine vertically or horizontally. For electricity price forecasting, Uniejewski et al. (2019) and Marcjasz et al. (2020) find that vertical averaging is more accurate, while Uniejewski and Weron (2021) obtain better results for horizontal averaging, with vertical averaging leading to CDFs that are too wide. For forecasting wave height, Taylor and Jeon (2018) report that vertical and horizontal averaging deliver similar accuracy. The fact that horizontal averaging delivers a CDF with lower variance than vertical averaging leads Bamber et al. (2016), Colson and Cooke (2017) and Cooke (2022) to express concern that horizontal averaging can result in a distribution that is too narrow. Using data from multiple studies in a variety of applications involving expert judgments of probability distributions, they find vertical averaging noticeably more accurate than horizontal averaging.

In some applications, only a set of quantile forecasts are available (see, for example, Makridakis et al. 2022). Indeed, this is the case with our Covid dataset. In such situations, Cooke et al. (2021) and Cooke (2022) acknowledge that horizontal averaging is easier, as vertical averaging requires a method to impute the complete CDF forecasts from the quantile predictions. Despite this, they warn against horizontal averaging, citing its tendency to lead to CDFs that underestimate the uncertainty.

2.3. Other Forms of Vertical and Horizontal Combining

Instead of using the simple average, distributional forecasts are often combined using weighted linear combinations. The vertical weighted combination $F_{V,w}$ and horizontal weighted combination $F_{H,w}$ are expressed as follows,

$$F_{V,w}(x) = \sum_{i=1}^k w_i F_i(x) \quad \text{and} \quad F_{H,w}^{-1}(\alpha) = \sum_{i=1}^k w_i F_i^{-1}(\alpha)$$

where the w_i are the combining weights. To ensure that the result is a well-defined CDF, vertical combining requires convex weights, i.e., $w_i \geq 0$ and $\sum_{i=1}^k w_i = 1$, while horizontal combining requires only that the weights are nonnegative. It is natural for the weights to reflect relative accuracy. For example, they can be optimized with the objective function set as a scoring rule, such as the log score or continuous ranked probability score (CRPS) (see, for example, Hall and Mitchell 2007; Raftery et al. 2005). The vertical weighted combination is sometimes termed the linear opinion pool (Stone 1961), and has been described as the most popular approach to combining distributional forecasts (Knüppel and Krüger 2022), with equal weighting viewed as a special case. Using weights in proportion to the log score of each forecast, Busetti (2017) finds that horizontal combining is more accurate than vertical combining for quarterly economic growth and inflation. In a weighted horizontal combining method, Taylor and Taylor (2023) set the weights to be inversely proportional to an approximation to the CRPS. If a different weighting scheme is considered desirable for different parts of the distribution (see, for example, Kapetanios et al. 2015; Fakoor et al. 2023), restrictions or adjustments would be needed to avoid quantile crossing (Chernozhukov et al. 2010).

The tendency for vertical combining to deliver overdispersed distributional forecasts has motivated nonlinear forms of vertical combining. The logarithmic opinion pool, which can be viewed as a geometric weighted average of PDFs, has been considered (see, for example, Busetti 2017; Cooke 2022). Building on this, Gneiting and Ranjan (2013) introduce generalized linear combinations, which involve a linear combination of CDF forecasts that have each been transformed using a link function. They also propose a beta-transformed linear pool that enables the combined CDF forecast to have a flexible variance, controlled by optimizing the parameters of the beta transformation. van der Meer et al. (2024) introduce CRPS-based online learning for this form of combining.

Jose et al. (2014) use trimming to control the variance of the CDF resulting from vertical averaging. They suggest entire CDF forecasts can be trimmed based on the mean, or the trimming can be performed separately, in a vertical sense, for different values of the outcome variable. After trimming, the remaining CDF forecasts are vertically averaged. Their exterior trimming approach reduces the impact of outlying CDFs to reduce the variance of the resulting CDF, while their interior trimming approach has the opposite effect by reducing the impact of central lying CDFs. Grushka-Cockayne et al. (2017a) apply these ideas to the CDFs produced in ensemble learning.

3. Angular Combining of Distributional Forecasts

3.1. Angular Averaging

With arguments in favor of both vertical and horizontal averaging, it becomes an empirical question as to which of the two approaches should be chosen for any given application. However, it could well be that neither vertical or horizontal averaging is ideal, and that there are useful aspects of each approach. For example, the unknown true density may be represented well by the tails produced by horizontal averaging and the central part of the distribution produced by vertical averaging.

In this paper, we propose an alternative averaging approach that allows the user to consider a range of possibilities between horizontal and vertical averaging. Our pragmatic alternative is to average on an angle that lies between these two extremes. We term this *angular averaging*. Figure 3(a) illustrates the idea with averaging of the same two CDFs considered in Figures 1 and 2. Figure 3(a) shows angular averaging performed on a line that has been rotated clockwise by an angle θ from the horizontal. Horizontal and vertical averaging are special cases of angular averaging, corresponding to θ being 0° and 90° , respectively. Figure 3(a) shows horizontal, vertical and angular averaging performed from the point indicated by the white star on the left CDF. The three different forms of averaging each lead to averaging of this point with a different point on the right CDF. The result is three different averages, shown by the white-filled, grey and black circular points.

Figure 3 Angular, horizontal and vertical averaging of points on two Gaussian CDFs in (a), and illustration of our parameterization in (b).

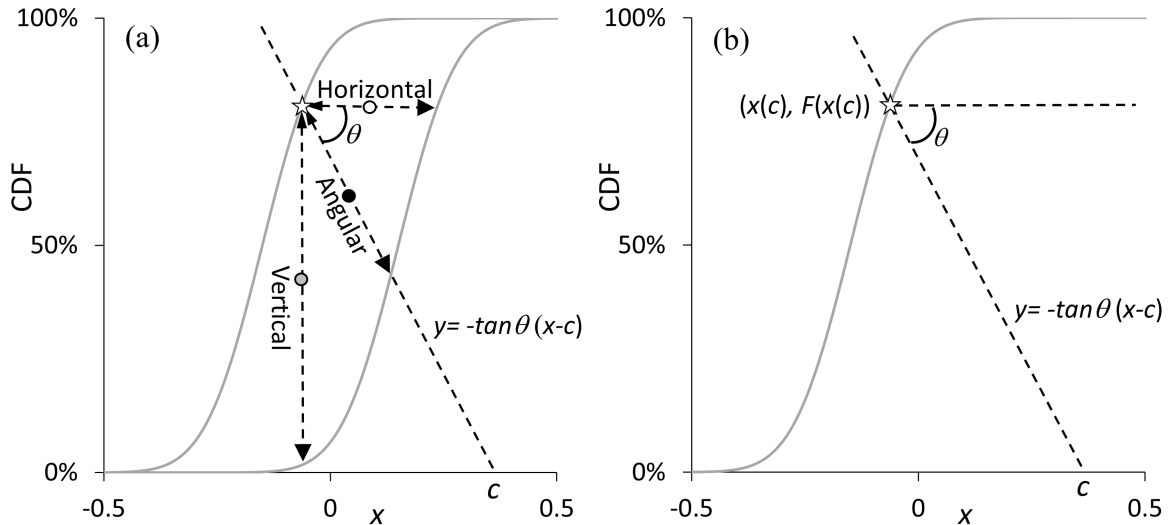


Figure 3(b) illustrates our parameterization for angular averaging. For a fixed $\theta \in (0^\circ, 90^\circ)$, consider a family of straight lines $y = -\tan\theta(x - c)$, where $-\tan\theta$ and $c \in (-\infty, \infty)$ are the gradient and x -intercept, respectively. We use c to parameterize each CDF, and to enable a formal description of the CDF resulting from angular averaging. For any given CDF F , we define the point of intersection between the CDF curve $y = F(x)$ and the line $y = -\tan\theta(x - c)$ as $(x(c), F(x(c)))$. The function $x(c)$ is increasing w.r.t. c , and $(x(c), F(x(c)))$ covers the entire CDF as c ranges from $-\infty$ to ∞ . Thus, the set of points $(x(c), F(x(c)))$ provides a parameterization of the CDF using c . That is, each point on the CDF can be uniquely identified by a single value of c . Indeed, $F(x(c))$ is a function of c that behaves as a CDF.

Using this parameterization for each of k CDFs, F_i , we have k points of intersection $(x_i(c), F_i(x_i(c)))$ between the CDFs and the line $y = -\tan\theta(x - c)$. Averaging the k points $\left(\frac{1}{k} \sum_{i=1}^k x_i(c), \frac{1}{k} \sum_{i=1}^k F_i(x_i(c))\right)$ yields the CDF $F_{A,\theta}$ of the angular average at $\frac{1}{k} \sum_{i=1}^k x_i(c)$,

$$F_{A,\theta} \left(\frac{1}{k} \sum_{i=1}^k x_i(c) \right) = \frac{1}{k} \sum_{i=1}^k F_i(x_i(c)) \quad (3)$$

We note that (3) contains $\frac{1}{k} \sum_{i=1}^k x_i(c)$ and $\frac{1}{k} \sum_{i=1}^k F_i(x_i(c))$, which represent horizontal and vertical averaging, respectively, implying that both of these forms of averaging are present in angular averaging. The PDF $f_{A,\theta}$ of the angular average is provided by Proposition 1. The proof of this proposition is presented in Online Appendix A. If $\theta = 0$, $f_{A,\theta}$ reduces to harmonic averaging of the PDFs, as in (2) for horizontal averaging. As θ increases and approaches 90° , implying all the $x_i(c)$ take the same value, $f_{A,\theta}$ converges to the arithmetic average of the PDFs, as in (1) for vertical averaging.

PROPOSITION 1. $f_{A,\theta} \left(\frac{1}{k} \sum_{i=1}^k x_i(c) \right) = \left(\sum_{i=1}^k \frac{f_i(x_i(c))}{f_i(x_i(c)) + \tan\theta} \right) / \left(\sum_{i=1}^k \frac{1}{f_i(x_i(c)) + \tan\theta} \right)$.

We also note that, although our parameterization is w.r.t. the x -intercept c of the angled line, we could have chosen to parameterize w.r.t. the y -intercept of this line. Indeed, this would be needed for horizontal averaging, as there is no x -intercept when the angled line is horizontal.

We have two comments to make regarding the angle θ . Firstly, if and only if θ is an angle in the range $[0^\circ, 90^\circ]$, will the function resulting from angular averaging be guaranteed to be monotonic

and take values in the range $[0,1]$, which are the necessary conditions for a CDF. If θ was not a value in the range $[0^\circ, 90^\circ]$, the angled line in Figure 3 could be crossed more than once by one of the CDFs to be combined. A second comment regarding the angle θ is that it is a parameter that should, ideally, be estimated using historical data. For many applications, past data is available, and so the estimation of a single parameter is not particularly burdensome. Indeed, the need for parameter estimation is also an aspect of many other combining methods. Furthermore, even though horizontal and vertical averaging require no parameter estimation, to decide which of these two methods to use, there is a need for a sample of past data with which to compare historical accuracy.

Figure 4 shows the CDF, and corresponding PDF, resulting from angular averaging of the same two Gaussian CDFs considered in Figures 1 to 3. The averaging has been performed at an angle of 45° , as conveyed by the dashed lines in Figure 4(a). For a variety of different values of θ , Figure 5(a) shows the different CDFs that result from angular averaging of the two Gaussian CDFs. Figure 5(b) provides the corresponding PDFs resulting from angular averaging. As we noted when discussing Figures 1(b) and 2(b), the PDFs resulting from vertical and horizontal averaging of the two Gaussian CDFs are bimodal and unimodal, respectively. It is interesting to note that, for the example we are using, it is only when θ exceeds about 85° that the angular averaging of the two CDFs leads to a PDF that is bimodal. This suggests that it would be wise in empirical studies to implement angular averaging for different values of θ spanning the full range from 0° to 90° . In our empirical studies of Sections 5 and 6, as candidate values for θ , we considered each integer value from 0° to 90° .

Figure 4 Angular combining (in black) of two Gaussian CDFs (in grey) in (a), and corresponding PDFs in (b). Averaging is performed at an angle $\theta = 45^\circ$, as indicated by the dashed lines.

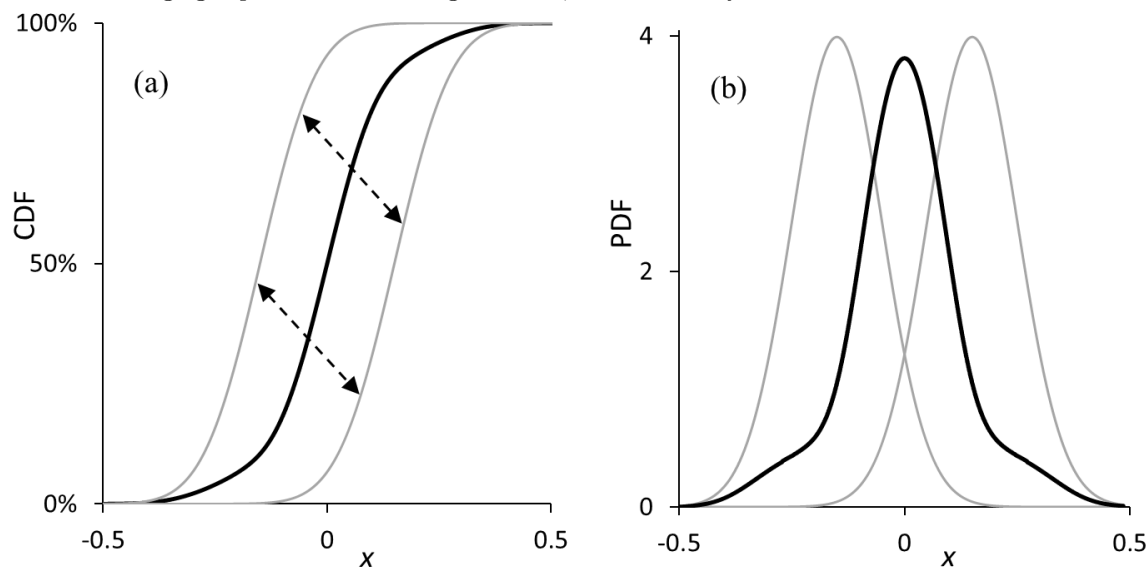
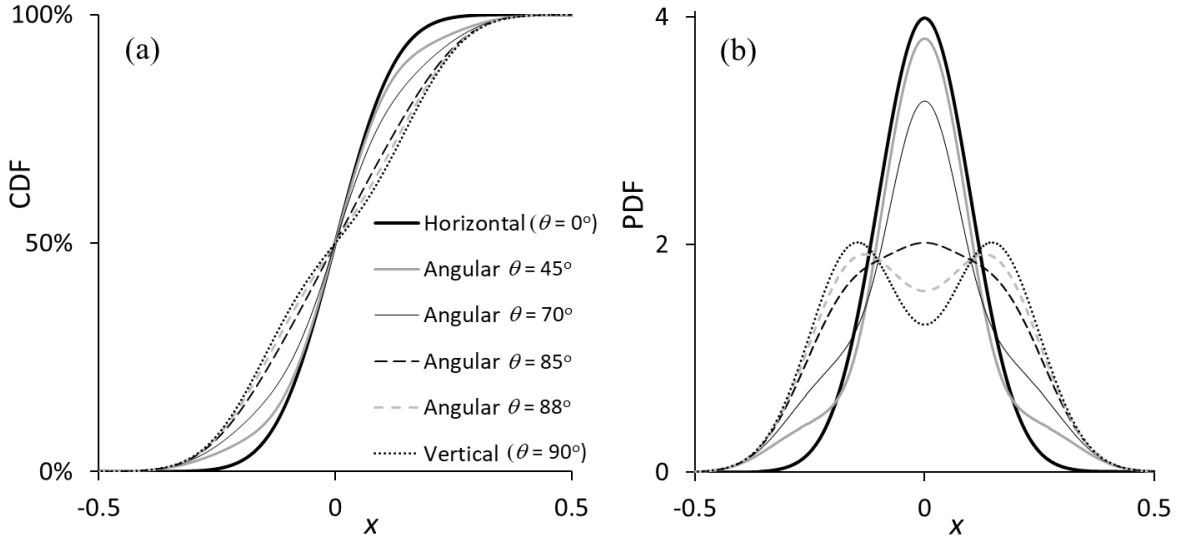


Figure 5 Horizontal, vertical and angular averaging of two Gaussian CDFs. Angular averaging performed for $\theta = 45^\circ, 70^\circ, 85^\circ$ and 88° . CDFs in (a) and PDFs in (b).



In Section 2.1, we commented that horizontal combining cannot be applied if any part of an individual CDF forecast is horizontal. We note that this is not a limitation of angular combining. Indeed, for $0^\circ < \theta < 90^\circ$, angular combining can be applied to individual CDF forecasts of any type, provided each is a well-defined CDF.

3.2. Other Forms of Angular Combining

In comparing horizontal, vertical and angular combining, we have focused on the simple average. However, CDFs have been combined horizontally and vertically using other approaches, as we discussed in Section 2.3. We suggest that such methods can be applied on an angle. As an example, in our empirical study of Section 5, we consider a combining method that weights forecasts inversely proportional to the CRPS, and implement this horizontally, vertically and at angles between 0° and 90° . Using the parameterization of Section 3.1, angular weighted combining is written as

$$F_{A,w,\theta} \left(\sum_{i=1}^k w_i x_i(c) \right) = \sum_{i=1}^k w_i F_i(x_i(c)). \quad (4)$$

3.3. Angular Combining as Generalized Linear Combining

A useful way to understand angular combining is through the framework of the generalized linear combination in (5), considered by Gneiting and Ranjan (2013),

$$h(F_{GL,w,h}(x)) = \sum_{i=1}^k w_i h(F_i(x)) \quad (5)$$

where h is a continuous and strictly increasing link function. In simple terms, the transformed CDF $F_{GL,w,h}$ under h is the vertical combination of the transformed F_i under h . Angular combining can be viewed as similar in spirit, but with the notable difference that a particular link function is used, and it is applied to the quantiles instead of the CDFs. We illustrate this in Figure 6 for the angular averaging of two CDFs in light grey, F_1 and F_2 . The figure shows F_1 and F_2 transformed horizontally to give two new CDFs in dark grey, $h_\theta(F_1)$ and $h_\theta(F_2)$, using the link function h_θ in (6), which defines a quantile transformation,

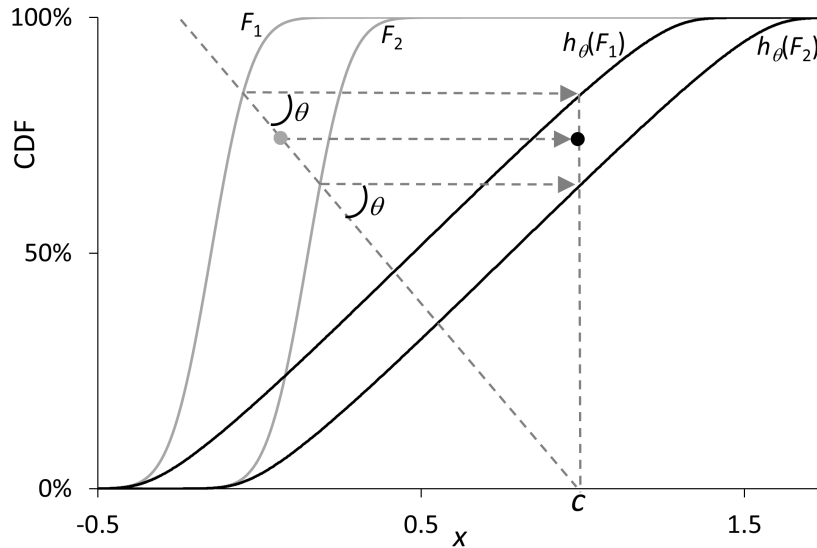
$$h_\theta(F)^{-1}(\alpha) = F^{-1}(\alpha) + \frac{\alpha}{\tan \theta} \quad \forall \alpha \in [0, 1]. \quad (6)$$

In Figure 6, the light grey point on the angled line is the angular average of the points of intersection of the angled line with F_1 and F_2 . The transformation of this light grey point results in the black point, which is also the vertical average of $h_\theta(F_1)$ and $h_\theta(F_2)$ at $x = c$, where c is the x -intercept of the angled line, as defined in Section 3.1. Based on this, we can reinterpret the angular combining in (4) within a framework similar to (5),

$$h_\theta(F_{A,w,\theta})(c) = \sum_{i=1}^k w_i h_\theta(F_i)(c). \quad (7)$$

In Online Appendix B, we discuss how (6) and (7) allow us to view angular combinations, like vertical and horizontal combinations, as barycenters of the set of individual CDF forecasts.

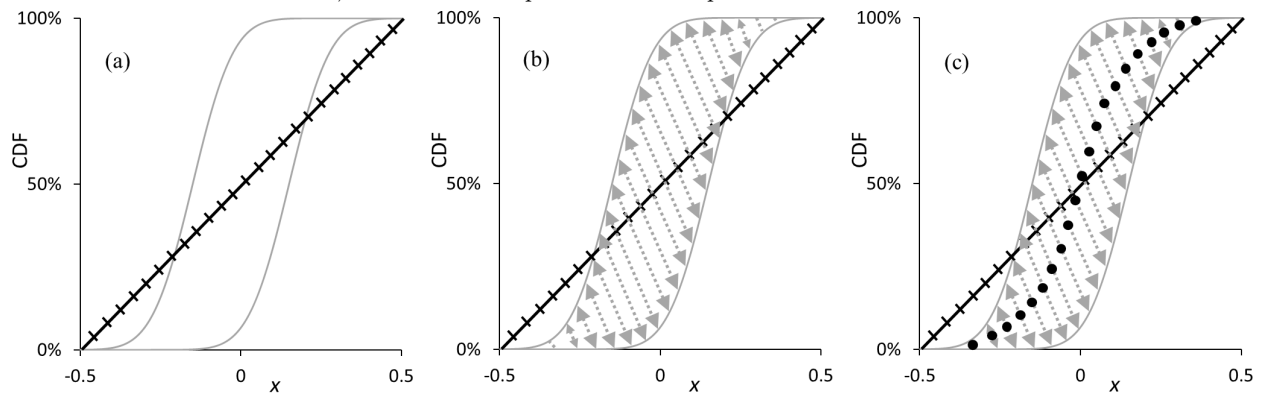
Figure 6 Visual illustration of angular averaging as generalized linear averaging. The light grey point is the angular average of the points of intersection of the angled line with the two CDFs, F_1 and F_2 . The transformation of this light grey point results in the black point, which is also the vertical average of the two transformed CDFs, $h_\theta(F_1)$ and $h_\theta(F_2)$, at the point $x = c$.



3.4. Practical Implementation of Angular Combining

To implement angular combining, we propose two numerical approaches. The first is a simple pragmatic approach based on the geometrical interpretation in Figure 3. In essence, it involves identifying the intersection points of the angled line $y = -\tan\theta(x - c)$ with each CDF F_i , and then computing the weighted average of the points of intersection for each value of c . Note that the intersection of each angled line with each CDF typically lacks a closed-form solution, thus necessitating a numerical method to determine the intersection point. To convey how we implemented this approach in our empirical analysis, Figure 7 provides an illustration for angular averaging at angle $\theta = 65^\circ$ using the same two Gaussian CDFs averaged in our previous figures. Notice that we have scaled the x -axes so that they each have unit length. This enables us to compare more easily values of the angle used for applications to different data. For CDFs with unbounded support, we would pragmatically suggest the scaled x -axis of unit length extends to at least the 1% and 99% quantiles of each CDF.

Figure 7 Implementation of angular averaging of two Gaussian CDFs. In (a), a diagonal straight line is drawn (in black), and on it are marked many evenly spaced points. Our empirical work used 1001 such points. In (b), an angled straight line at angle $\theta = 65^\circ$ is drawn (in grey) through each marked point and between the two CDFs. In (c), the midpoint of each angled straight line is obtained, and these midpoints map out the new CDF, with linear interpolation used to produce the full continuous CDF.



The second approach to implementation is a simulation algorithm for generating randomly sampled values for the distribution produced by angular combining. An appeal of this approach is that it avoids the need to solve implicit equations to find the points of intersection of the angled lines with the CDFs, which is required in the pragmatic approach of Figure 7. The simulation algorithm is described in Online Appendix C, and available in an R package at: <https://github.com/XiaochunMeng1/R-package-for-Angular-Combining>.

4. Theoretical Results

In this section, we present results concerning the mean, variance, intervals and CRPS of the distributional forecast resulting from angular combining. We also consider the distribution produced by an angular form of median aggregation. All proofs are provided in Online Appendix A.

4.1. Mean of Angular Combining

Lichtendahl et al. (2013) show that, for vertical and horizontal averaging, the means of their resulting CDFs both equal the average of the means of the individual CDFs. They explain that this is an attractive property because the mean of a CDF forecast is widely used as a point forecast, and averaging is often a successful approach to aggregating point forecasts. The property is not possessed by many other methods for combining CDF forecasts, such as median aggregation and the logarithmic opinion pool. It is, therefore, interesting that angular averaging possesses this property. This is implied by Proposition 2, which considers the general case of weighted combining.

PROPOSITION 2. For horizontal, vertical and angular combining, with any set of weights $\{w_1, \dots, w_k\}$, the mean of the combination is identical to the weighted average of the means of the individual CDFs F_i in the combination.

In empirical studies, CDF forecast accuracy is often heavily influenced by the location of the CDF forecasts. A practical implication of the combining methods delivering CDFs with the same mean is that their relative accuracy will be due to other aspects of the CDF, such as the variance.

4.2. Variance of Angular Combining

Lichtendahl et al. (2013) prove that the horizontal average has lower variance than the vertical average. Theorem 1 extends this result to angular combining, of which angular averaging is a special case.

THEOREM 1. For any set of weights $\{w_1, \dots, w_k\}$, the angular combination $F_{A,w,\theta}$ has lower variance than the vertical combination $F_{V,w}$.

Theorem 1 implies that the angular and horizontal combinations both have lower variance than the vertical combination. In fact, it is straightforward to extend the proof of this theorem regarding variance to higher even (central) moments. As angular combining conceptually lies between vertical and horizontal combining, it is natural to ask whether the variance of the angular combination falls between the variances of the vertical and horizontal combinations. While this may not hold generally, we now explain that it is true in the specific scenario described in Assumption 1.

ASSUMPTION 1. *Each individual distribution F_i in the combination has the same scale and is from the same location-scale family, where the PDF of the standardized member of the location-scale family is symmetric about 0 and unimodal.*

These assumptions are among those adopted in Proposition 5 of Lichtendahl et al. (2013), which compares the CDFs for vertical and horizontal averaging. Our Lemma 1 below extends the proposition to the angular averaging of two CDFs.

LEMMA 1. *Under Assumption 1, when two distributions are averaged, the PDF $f_{A,\theta}$ of angular averaging is symmetric about its mean, and $F_{A,\theta}(x)$ is increasing w.r.t. θ when x is below the mean, and $F_{A,\theta}(x)$ is decreasing w.r.t. θ when x is above the mean.*

Theorem 2 builds on Lemma 1 to show that the variance of the angular combination $F_{A,w,\theta}$ is increasing w.r.t. the angle θ , regardless of the number of CDFs included in the combination.

THEOREM 2. *Under Assumption 1, for any set of weights $\{w_1, \dots, w_k\}$, the variance of the angular combination $F_{A,w,\theta}$ is increasing w.r.t. θ , with the implication that the horizontal combination has lower variance than the angular combination, which has lower variance than the vertical combination.*

Proposition 2 and Theorem 2 lead to practical guidance on selecting the best combining method w.r.t. the mean and variance, under Assumption 1. Using historical data, we first set the mean by obtaining the weights w_i , and then perturb θ to target the variance. The weights can be optimized using a point forecast combining method, or, as in our empirical study, pragmatically set to be inversely proportional to the CRPS. Once the weights are determined, we produce the CDF forecasts from vertical and horizontal combining for each historical period. If the variances of both are too high

for the past data, horizontal combining should be used; if the variances of both are too low, vertical combining is recommended; and if the variances of the CDFs produced by horizontal combining are too low, while the variances of the CDFs from vertical combining are too high, there exists a value of θ for which angular combining delivers the CDF forecasts with most accurate variances.

4.3. Interval Forecasts from Angular Averaging

In this section, we consider the interval forecasts, containing the medians, obtained from the CDFs produced by the different combining approaches. Lichtendahl et al. (2013) show that under Assumption 1, if the means μ_i of individual predictions are symmetrically located around the common mean of the horizontal and vertical averages, horizontal averaging results in a narrower interval compared to vertical combining. Proposition 3 extends this, showing that the interval forecasts of horizontal averaging are also narrower than those for angular averaging.

PROPOSITION 3. *Let $\alpha_1 < 0.5$ and $\alpha_2 > 0.5$ denote two arbitrary probability values. Under Assumption 1, if the μ_i are symmetrically located around the common mean of the horizontal and angular averages, we have $(F_H^{-1}(\alpha_1), F_H^{-1}(\alpha_2)) \subseteq (F_{A,\theta}^{-1}(\alpha_1), F_{A,\theta}^{-1}(\alpha_2))$.*

Proposition 4, as a direct consequence of Lemma 1, provides a stronger result when two CDFs are averaged. In this case, vertical and horizontal averaging produce the widest and narrowest prediction intervals, respectively, while angular averaging yields intervals that fall between the two,

PROPOSITION 4. *Let $\alpha_1 < 0.5$ and $\alpha_2 > 0.5$ denote two arbitrary probability values. Under Assumption 1, the interval forecast for the angular average of two CDFs expands as the angle θ increases, i.e., $(F_{A,\theta_1}^{-1}(\alpha_1), F_{A,\theta_1}^{-1}(\alpha_2)) \subseteq (F_{A,\theta_2}^{-1}(\alpha_1), F_{A,\theta_2}^{-1}(\alpha_2))$ if $\theta_1 \leq \theta_2$.*

This proposition can be used as the basis for similar practical guidance to that presented in Section 4.2, with the best choice between horizontal, vertical and angular averaging dictated by the interval forecasts derived from the CDF forecasts produced by horizontal and vertical averaging. We note that, in comparison with the intervals of the data generating process (DGP), wider intervals can be viewed as indicating underconfidence, while narrower intervals imply overconfidence (see, for example, Moore and Healy 2008, Lichtendahl et al. 2013, Soll et al. 2023).

4.4. Scoring Rules and Angular Combining

Let Z denote the random variable of the DGP, and let G denote its CDF. A scoring rule $S(F, z)$ assigns a numerical score to a CDF forecast F and a realization z , and is *proper* if its expectation is minimized when F coincides with G . Hence, proper scoring rules, such as the CRPS, incentivize honest reporting by forecasters. The *divergence* of a proper scoring rule is defined as $\mathbb{E}[S(F, Z)] - \mathbb{E}[S(G, Z)]$ (Gneiting and Raftery 2007). The divergence is a nonnegative quantity that measures the ‘distance’ between F and G , with a smaller value indicating superior accuracy. By contrast with variance and interval forecasts, which are inherent properties of a CDF forecast, the value of a score depends on the DGP, making it impossible to determine the best model without knowledge of the DGP. Nevertheless, we can still make the meaningful observation that, as angular combining encompasses both horizontal and vertical combining, given sufficient data to estimate θ , angular combining will not be outperformed by horizontal or vertical combining for any proper score, i.e., these combining methods have greater ‘distance’ from the true DGP than angular combining.

Lichtendahl et al. (2013) show that the score for vertical averaging is no greater than the average of the scores of the individual distributions for the linear score, log score, quadratic score and CRPS. They show that this is also true for the linear and log scores when it comes to horizontal averaging. Although, for the quadratic score, the result is not necessarily valid for horizontal averaging, the authors establish conditions under which it is true. They do not discuss the result for horizontal averaging for the CRPS. Theorem 3 addresses this, and extends the result to angular combining. Before providing the theorem, we define the CRPS, with $\mathbb{1}(\cdot)$ representing the indicator function,

$$CRPS(F, z) = \int_{-\infty}^{\infty} (F(x) - \mathbb{1}(x > z))^2 dx.$$

THEOREM 3. *For any set of weights $\{w_1, \dots, w_k\}$, the CRPS for the horizontal and angular combinations are less than or equal to the weighted combination of the CRPS of the individual distributional forecasts F_i in the combination.*

This theorem indicates that angular averaging captures the wisdom of the crowd by providing “accuracy that is no worse than the average member of the crowd” (Larrick et al. 2012; Lichtendahl

et al. 2013). A further practical implication of Theorem 3 is that angular combining cannot be outperformed, in terms of the CRPS, by the weakest individual CDF forecast. The theorem also has practical relevance for numerically optimizing the combining weights based on the CRPS, because it ensures that any local minimum is also the global optimum. Consequently, one can initialize the numerical procedure with a set of arbitrary weights and employ a local optimization technique to obtain the optimal weights.

4.5. Angular Median Aggregation

Hora et al. (2013) show that performing median aggregation horizontally and vertically results in the same CDF. They find that, although for a set of calibrated individual CDF forecasts, median aggregation will deliver a CDF that is not calibrated and is overdispersed, the miscalibration is less than with vertical averaging. The approach has the appeal of robustness and computational simplicity, which motivates consideration of an angular form of median aggregation.

Similarly to angular averaging, the median can be obtained at any angle θ . In other words, to construct the angular median CDF for a chosen θ , we find the median of the points of intersection of the individual CDFs with an angled line $y = -\tan\theta(x - c)$, and repeat this for different values of $c \in (-\infty, \infty)$. Theorem 4 shows that, if there is an odd number of individual CDFs, the same CDF is produced when the median is obtained vertically, horizontally or at an angle.

THEOREM 4. When k is odd, obtaining the median of k CDFs, horizontally, vertically or at an angle θ produces the same CDF.

5. Empirical Study of Covid Mortality Forecasting

In this section, we use mortality data to evaluate our proposed approach to distributional forecast combining.

5.1. The Dataset

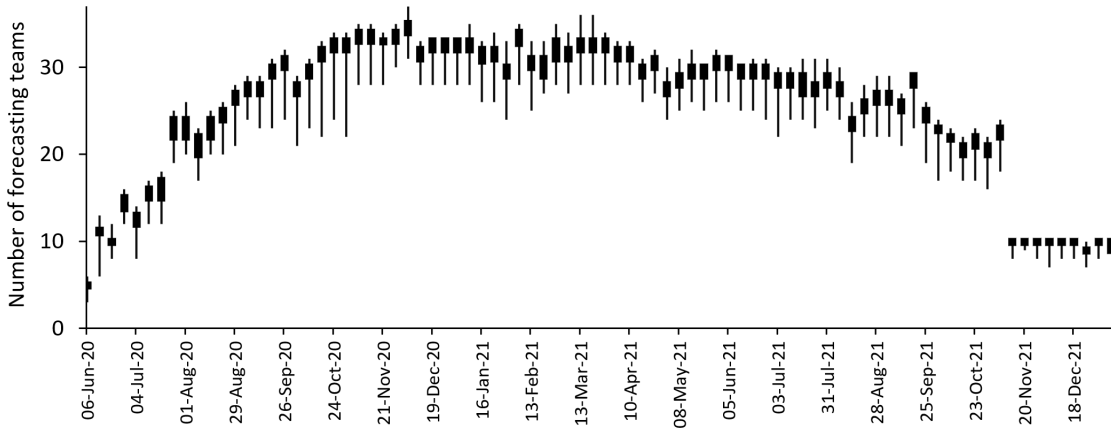
We used data from the COVID-19 Forecast Hub (<https://covid19forecasthub.org/>). The Hub provides open access to weekly observations and forecasts from multiple forecasting teams for one

to four weeks-ahead for the number of reported Covid deaths at the national and state level in the U.S. Mortality forecasts were used by public health decision makers during the pandemic (Adam 2020; Ray et al. 2023). Forecasts from the Hub gained widespread attention with weekly updates presented on the website of the Center for Disease Control and Prevention. The teams submitting forecasts to the Hub came from academia, industry and government affiliated groups. We used forecasts of the number of weekly Covid deaths produced from the 84 weekly forecast origins from 6 June 2020 to 8 January 2022, inclusive, and mortality observations, recorded on 15 January 2022, for the weeks ending 13 June 2020 to 15 January 2022, inclusive. We considered mortality at the national level, for the 50 states, and for the District of Columbia, which for simplicity we refer to as a state. The dataset, therefore, involved 52 time series. Taylor and Taylor (2022) used the same data in a study of interval forecast combining.

The curators of the Hub invited forecasting teams to submit a point forecast and quantile forecasts corresponding to the following 23 probability levels: 1%, 2.5%, 5%, 10%, 15%, 20%, 25%, 30%, 35%, 40%, 45%, 50%, 55%, 60%, 65%, 70%, 75%, 80%, 85%, 90%, 95%, 97.5% and 99%. As our interest in this paper is in distributional forecasts, we constructed continuous CDFs from the 23 quantiles. To do this, we used the following simple approach: we defined the lower bound of the distribution as being a distance below the 1% quantile equal to the difference between the 1% and 2.5% quantiles (unless this resulted in a negative lower bound, in which case we set it to be zero); we defined the upper bound of the distribution as being a distance above the 99% quantile equal to the difference between the 97.5% and 99% quantiles; and we used linear interpolation to give the CDF between each pair of quantiles, between the lower bound and the 1% quantile, and between the 99% quantile and the upper bound. (Defining the lower and upper bounds as the 1% and 99% quantiles, respectively, produced very similar out-of-sample results for the evaluation measures we describe in Section 5.2.) Each week, the curators of the Hub generated an “ensemble” forecast combination. Initially, the ensemble was the horizontal average; from mid-July 2020, it was computed as the median; and after mid-November 2021, it was a horizontal weighted combination. At each forecast origin, for each series, the curators of the Hub screened forecasting teams for inclusion in their

ensemble, removing teams if their forecasts were clearly unrealistic. We followed the same approach, so that, for each forecast origin and series, we included in combinations only the teams considered eligible by the Hub curators for that forecast origin and series. There was variation over time in the identity and number of teams. In Figure 8, for each forecast origin, a box plot summarizes the differing number of eligible teams for each of the 52 series. About half the teams used compartmental models. The others employed statistical methods, machine learning or agent-based models. The diversity of methods motivates attempts to extract wisdom from the crowd (see Surowiecki 2004).

Figure 8 For each of the 84 forecast origins in the Covid dataset, the box plot summarizes the number of eligible forecasting teams for each of the 52 series.



5.2. Structure of the Study and Evaluation Measures

We used forecasts made from the first 10 out of the 84 forecast origins for the initial in-sample parameter estimation. For the remaining 74 forecast origins, we used an expanding in-sample period consisting of all weeks up to and including the origin itself. Out-of-sample forecasts were, therefore, produced for the final 74 weeks of each of the 52 mortality time series. Our choice of just 10 periods for the initial estimation sample was driven by the desire for a reasonably long out-of-sample period.

We used the following multiple quantile score (MQS) to assess distributional forecast accuracy,

$$MQS(F, z) = \frac{1}{23} \sum_{i=1}^{23} 2QS(F^{-1}(\alpha_i), z) \quad \text{where} \quad QS(F^{-1}(\alpha_i), z) = (\alpha_i - \mathbb{1}(z \leq F^{-1}(\alpha_i))) (z - F^{-1}(\alpha_i)).$$

z is the observation, F is the CDF, and $F^{-1}(\alpha_i)$ is the quantile with probability level α_i , which we set as the 23 probability levels chosen by the Hub curators. QS is the widely-used score for

a quantile, which is also known as the *pinball* or *check* loss function. The MQS is a proper score for the distribution (Grushka-Cockayne et al. 2017b; Jose and Winkler 2009). It approximates the CRPS. We use the MQS rather than the CRPS itself, as the MQS is employed in other studies of the COVID-19 Forecast Hub data, which reflects the focus of the Hub on forecasting the 23 quantiles (see, for example, Bracher et al. 2021; Ray et al. 2023). In addition to the MQS, we also evaluated the QS for each of the 23 probability levels to provide insight into forecast accuracy for the different regions of the distributions.

In addition to averaging each score over the out-of-sample period, we also averaged over the lead times, as the relative performances of the methods were similar for the four lead times, and the series were relatively short. We report the scores averaged across all 52 series, but as this will be heavily influenced by the higher mortality series, we also report results for the following four groupings of the series: the U.S. national level series; the 17 states for which cumulative mortality was highest in the final week of the dataset; the 17 states with the next highest cumulative mortality in the final week; and the 17 states with lowest cumulative mortality in the final week.

We also computed skill scores, defined as the percentage by which a method is more accurate than a benchmark, which we chose to be vertical averaging. Skill scores provide a further way of avoiding higher mortality series dominating when averaging across series. To average over skill scores, we first calculated the geometric mean of the ratios of the score for each method to the score for the benchmark method, then subtracted this from 1, and multiplied the result by 100.

To evaluate unconditional calibration for the CDF forecasts, we used reliability diagrams, which convey calibration across the quantiles of the CDF.

5.3. Implementing Horizontal, Vertical and Angular Combining

We implemented horizontal, vertical and angular averaging, as well as horizontal, vertical and angular forms of performance-based weighted combining. As we discussed in relation to Figure 8, the identity and number of teams submitting forecasts to the Hub varied over time. In view of this, we pragmatically set each combining weight to be inversely proportional to the team’s in-sample MQS, which was one of the combining approaches considered in the horizontal combining study of

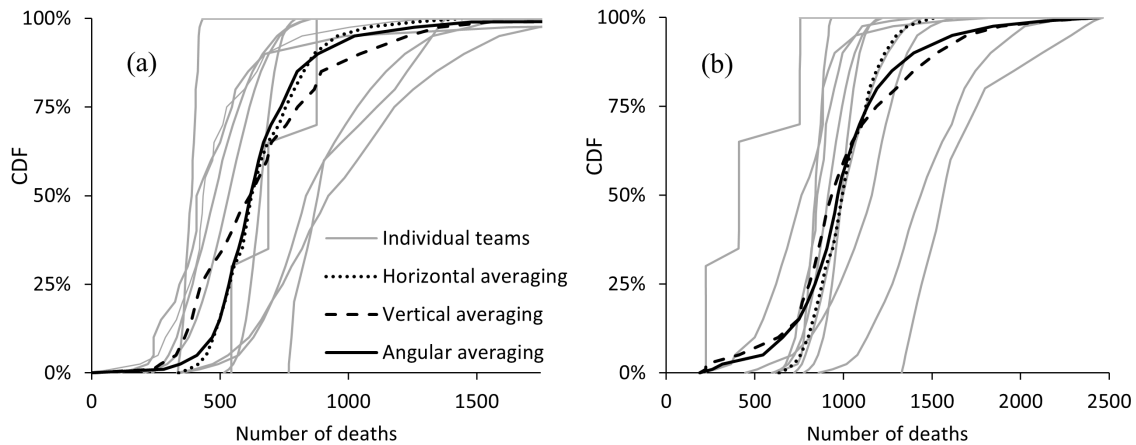
Taylor and Taylor (2023). If fewer than five past periods were available from which to produce the in-sample MQS for a team, the MQS was assumed equal to the average of the MQS of the other teams in the combination. Note that the weights only approximately reflect relative performance because the MQS will typically not have been computed from the same past periods for all teams, due to inconsistencies in the record of submissions among the teams.

Our implementation of horizontal averaging and horizontal weighted combining simply involved combining the quantile forecasts for each of the 23 probability levels. Vertical combining involved averaging and weighted combining of the probability forecasts for each of a set of values of the mortality variable. This set consisted of all 23 quantile forecasts submitted by all the teams.

To implement angular combining, we used the pragmatic numerical approach described in Section 3.4. This was adequate for our study because identifying the intersection points of each angled line with each CDF forecast was straightforward due to the CDF forecasts being piecewise-linear. In Figure 7 of Section 3.4, we described how, for angular averaging, the approach involved, for each of the $m=1001$ angled straight lines (in grey), averaging the points of intersection of the angled straight line with the CDF forecasts. For each angled straight line, in addition to averaging, we applied the performance-based weighted combination, using the same weights we had used for horizontal and vertical weighted combining. We then optimized the angle θ separately for angular averaging and angular weighted combining. For each series and method, at each forecast origin, we optimized θ by minimizing the in-sample MQS averaged over the four lead times, with the in-sample MQS for each lead time computed using only observations at or before the forecast origin.

Figure 9 provides examples of the CDF forecasts produced by the individual teams and by horizontal, vertical and angular averaging. The examples correspond to the forecasts produced from the final forecast origin in our dataset for California and New York State. For each state, the figure shows that the CDF forecasts of the teams vary quite considerably in terms of their location, spread and shape. We can also see differences between the CDFs produced by the three forms of averaging.

Figure 9 1 week-ahead CDF forecasts for Covid mortality in the week up to 15 January 2022 from 10 individual teams and the three averaging methods for (a) California, and (b) New York State. For angular averaging, the optimized angle θ was 60° for California and 79° for New York.



In a small number of cases, forecasting teams submitted CDF forecasts for which the quantiles were identical for two or more adjacent values of the 23 probability levels. For example, this is the case for the left-most CDF forecast in Figure 9(b). This is problematic for vertical combining because, for certain values on the x -axis, there is more than one CDF value. To address this, for any such value on the x -axis, we simply averaged the CDF values before applying vertical combining.

With optimization of the angle θ performed at each forecast origin, angular combining essentially allows switching between different angles as the method is passed through the out-of-sample period. To challenge this, we implemented a method that switched between horizontal and vertical combining, with the choice between these two combinations made, at each forecast origin, by selecting the one with lowest in-sample MQS. We call this *horizontal/vertical switching*. We implemented a version of this that switched between horizontal and vertical averaging, and, separately, a version that switched between horizontal and vertical weighted combining.

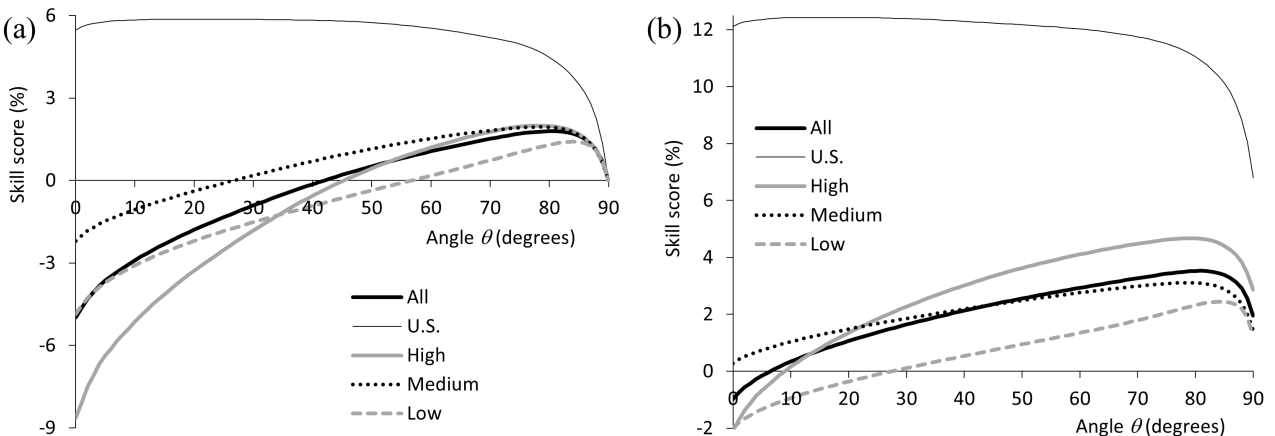
As our focus in this paper is horizontal, vertical and angular combining, we initially report results for only these methods. In Section 5.8, we present results for other combining methods.

Comparing the results of the combining methods with those of individual teams is difficult because none of the teams provided forecasts that passed the Hub's eligibility screening for all past periods and series. In view of this, we focus only on combining methods in our analysis.

5.4. Results for Angular Combining with a Fixed Angle

As an initial investigation into suitable values of the angle θ used in angular combining, we evaluated the accuracy of the approach when θ was not optimized but was fixed at the same value for all 74 forecast origins used to produce out-of-sample forecasts. We did this, in turn, for integer values of θ between 0° and 90° . For angular averaging, Figure 10(a) presents the resulting MQS skill scores, computed for the five categories of series: all 52 series, the U.S. national level series, and the high, medium and low mortality groupings of series. Higher values of the skill score are preferable. First note that the extreme right of the figure ($\theta = 90^\circ$) corresponds to vertical averaging, and as this is the benchmark method in the skill score calculation, the skill scores are all zero at this right extreme. The left extreme ($\theta = 0^\circ$) corresponds to horizontal averaging. For the U.S. national level series, the figure shows the skill score relatively high for values of θ up to about 70° , beyond which the skill score reduces to its lowest value at $\theta = 90^\circ$, indicating vertical averaging is not suitable for this mortality series. For the other four categories of series, the other four lines in Figure 10(a) show the skill score at its lowest when $\theta = 0^\circ$, indicating that angular averaging with any angle above 0° was more accurate than horizontal averaging. These four lines all peak with θ between about 80° and 85° , suggesting that angular averaging with an angle in this range would be suitable for series in these four categories, and that it would be more accurate than vertical averaging ($\theta = 90^\circ$). Figure 10(b) provides similar insight for angular weighted combining to that provided by Figure 10(a).

Figure 10 For the Covid dataset, MQS skill score for the out-of-sample period for angular averaging at different angles in (a), and for angular weighted combining in (b). Higher values of the skill score are better.



The message from Figure 10 that relatively high values for θ tended to be most suitable is interesting because, for the angular averaging of two Gaussian CDFs in Figure 5, an informal

conclusion could be that the CDF resulting from angular averaging only became very noticeably different to horizontal averaging for values of θ above about 70° . However, such a conclusion from Figure 5 ignores the tails of the distributions, which are noticeably different for much lower values of θ . It should also not be overlooked that Figure 10 presents the MQS, which summarizes accuracy for the full distribution. This motivates a more careful consideration of the tails of the distribution produced by angular averaging, and we do this using the quantile score in Section 5.7.

5.5. Optimized Values of the Angle

In practice, the angle θ would need to be estimated. In our empirical comparison of methods in Sections 5.6 to 5.8, we implemented angular averaging and angular weighted combining for each of the 52 series and 74 forecast origins used to produce out-of-sample forecasts. For each of these methods, we optimized the angle θ for each series and origin by minimizing the in-sample MQS. The histogram in Figure 11 summarizes the resulting optimized values of θ . The left extreme of the figure shows that angles close to the horizontal ($\theta = 0^\circ$) were quite often found to be optimal. However, the right end of the figure shows that the optimized angle was more frequently found to be closer to vertical ($\theta = 90^\circ$), with angles between about 70° and 90° often obtained.

Figure 11 For angular averaging and angular weighted combining, histogram of the angle θ optimized for the 52 Covid series at the 74 forecast origins.

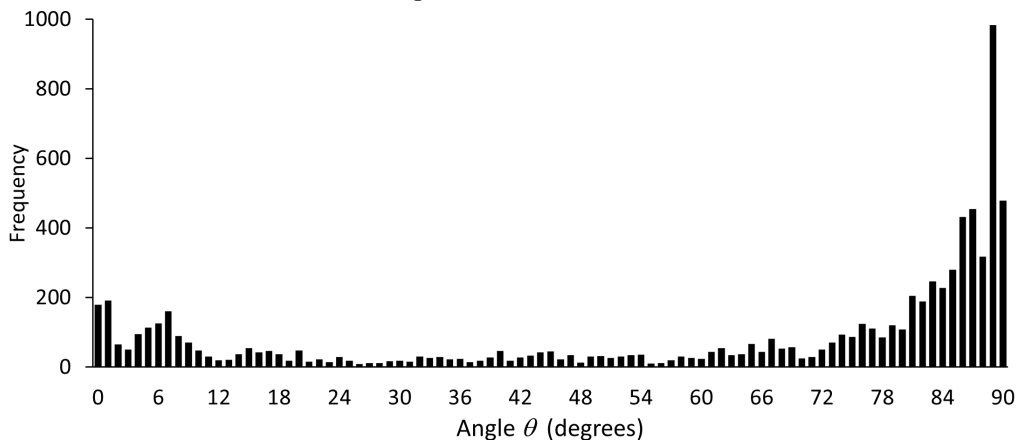
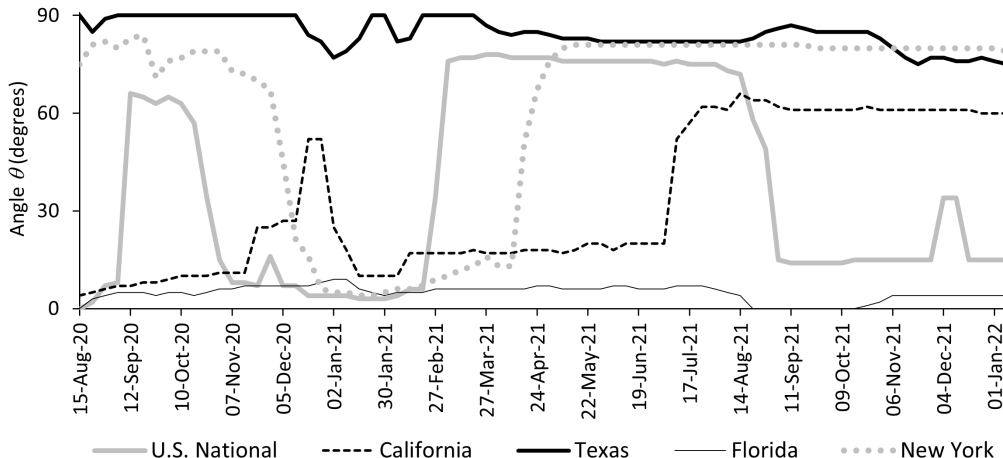


Figure 12 shows the angles optimized for each forecast origin for the five series for which mortality was highest in the final period of the dataset. The figure shows that for Florida and Texas, the optimized angles remained quite close to 0° and 90° , respectively, across the forecast origins. By

contrast the optimized angles for the other three series were generally not particularly close to the extremes of 0° and 90° .

Figure 12 For angular averaging, the optimized angle θ at the 74 forecast origins for five of the Covid series.



5.6. Comparing Horizontal, Vertical and Angular Combining using the MQS

In this section, we evaluate the out-of-sample performance of angular combining with optimized angle by comparing it with horizontal and vertical combining, as well as horizontal/vertical switching. Table 1 summarizes the MQS results. The first five columns of values provide the MQS for each of the five categories of the time series considered in Figure 10. Lower values of the MQS are better. The final five columns of Table 1 present the corresponding skill scores. In each column, bold highlights the best approach to averaging and the best approach to weighted combining. Looking at the averaging approaches in the first four rows, we see that horizontal averaging was the most accurate for the U.S. national level series and the poorest for the other four categories. The horizontal/vertical switching method performed well for the U.S. national level series because it selected horizontal averaging for all forecast origins. For the other four categories, the skill scores show that the switching method was not able to outperform vertical averaging. For these four categories, angular averaging was a little more accurate than vertical averaging. For weighted combining, we again see horizontal combining performing well only for the U.S. national level series, with angular combining again a little better than vertical combining overall. We also note that each form of weighted combining outperforms the corresponding form of averaging. In Online Appendix D.1, for the methods in Table 1, we present the skill scores for each of the 52 series.

Table 1 For the Covid dataset, MQS for the out-of-sample period for the three forms of combining and horizontal/vertical switching.

| | MQS | | | | | MQS skill score (%) | | | | |
|-------------------------------|--------------|-------------|-------------|------------|-------------|---------------------|------------|------------|------------|------------|
| | U.S. | High | Medium | Low | All | U.S. | High | Medium | Low | All |
| <i>Averaging</i> | | | | | | | | | | |
| Vertical | 949.1 | 69.2 | 27.7 | 8.2 | 52.6 | 0.0 | 0.0 | 0.0 | 0.0 | 0.0 |
| Horizontal | 897.3 | 80.1 | 28.5 | 8.5 | 55.5 | 5.5 | -8.6 | -2.2 | -4.9 | -5.0 |
| Horizontal/vertical switching | 897.3 | 69.8 | 27.9 | 8.2 | 51.9 | 5.5 | -1.3 | -0.7 | -1.3 | -1.0 |
| Angular | 903.3 | 68.5 | 27.5 | 8.2 | 51.5 | 4.8 | 1.0 | 0.9 | 0.1 | 0.8 |
| <i>Weighted combining</i> | | | | | | | | | | |
| Vertical | 884.5 | 67.1 | 27.3 | 8.1 | 50.5 | 6.8 | 2.9 | 1.4 | 1.2 | 2.0 |
| Horizontal | 834.1 | 75.2 | 28.0 | 8.2 | 52.5 | 12.1 | -2.1 | 0.3 | -2.0 | -1.0 |
| Horizontal/vertical switching | 834.1 | 67.3 | 27.6 | 8.1 | 49.7 | 12.1 | 3.1 | 1.0 | 0.0 | 1.6 |
| Angular | 839.1 | 66.6 | 27.2 | 8.1 | 49.4 | 11.6 | 4.0 | 2.4 | 1.1 | 2.7 |

Note: The unit of the score is deaths. Lower scores and higher skill scores are better. Skill scores use vertical averaging as benchmark. Bold indicates the best method in each column within the averaging block and within the weighted combining block.

In Section 4.1, we noted that the CDFs produced by horizontal, vertical and angular combining have the same mean if the same combining weights are used. This is useful because it implies that their relative performances in Table 1 are due to other aspects of the CDFs, such as their variance.

In some applications, data is not available to optimize combining method parameters. From Table 1, vertical or horizontal averaging could be used, although the choice between the two would need to be made subjectively. For angular averaging, when the angle θ cannot be optimized, a simple idea, informally lying midway between horizontal and vertical averaging, is to select $\theta = 45^\circ$. This would seem reasonable if the forecaster had no basis on which to choose between horizontal and vertical averaging. However, if they had prior experience with similar datasets, this could lead to a moderate preference for either horizontal or vertical averaging, in which case they could, perhaps, select $\theta = 22.5^\circ$ or $\theta = 67.5^\circ$, respectively. In view of Theorems 1 and 2, another approach would be to choose the angle θ that delivers a CDF with the desired standard deviation. For example, θ could be chosen so that σ_A is the average of σ_H and σ_V , where σ_A , σ_H and σ_V are the standard deviations of the CDFs produced by angular, horizontal and vertical averaging, respectively. If the forecaster has a view as to whether σ_H or σ_V is closer to the truth, then θ could, perhaps, be chosen so that $\sigma_A = 0.75\sigma_H + 0.25\sigma_V$ or $\sigma_A = 0.25\sigma_H + 0.75\sigma_V$, respectively. Table 2 compares the accuracy of these proposals. The table shows that angular averaging with $\theta = 45^\circ$ performed reasonably, but the best performing method was angular averaging with $\theta = 67.5^\circ$, confirming insight from Figure 10 that,

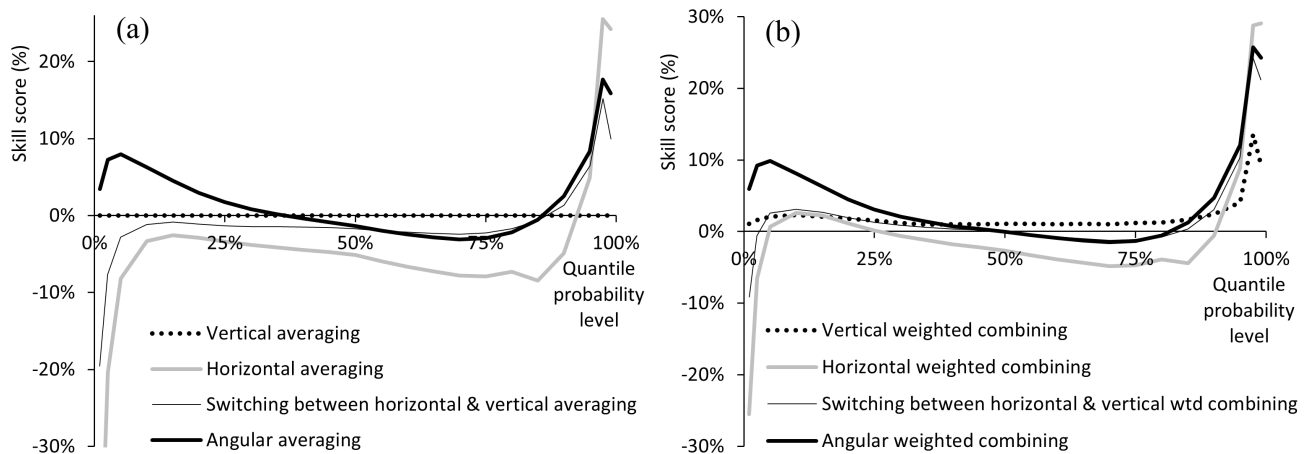
overall, angular averaging was, for this dataset, most accurate for values of the angle θ above about 45° .

Table 2 For the Covid dataset, MQS for the out-of-sample period for combining methods involving no parameter optimization.

| | MQS | | | | | MQS skill score (%) | | | | |
|--|--------------|-------------|-------------|------------|-------------|---------------------|------------|------------|------------|------------|
| | U.S. | High | Medium | Low | All | U.S. | High | Medium | Low | All |
| <i>Averaging (from Table 1)</i> | | | | | | | | | | |
| Vertical | 949.1 | 69.2 | 27.7 | 8.2 | 52.6 | 0.0 | 0.0 | 0.0 | 0.0 | 0.0 |
| Horizontal | 897.3 | 80.1 | 28.5 | 8.5 | 55.5 | 5.5 | -8.6 | -2.2 | -4.9 | -5.0 |
| <i>Angular averaging</i> | | | | | | | | | | |
| Angle $\theta = 22.5^\circ$ | 893.5 | 75.0 | 28.0 | 8.3 | 53.6 | 5.9 | -2.9 | -0.2 | -2.0 | -1.6 |
| Angle $\theta = 45^\circ$ | 894.1 | 72.4 | 27.7 | 8.2 | 52.6 | 5.8 | 0.0 | 0.9 | -0.6 | 0.2 |
| Angle $\theta = 67.5^\circ$ | 898.9 | 70.2 | 27.5 | 8.1 | 51.9 | 5.3 | 1.6 | 1.8 | 0.6 | 1.4 |
| $\sigma_A = 0.75\sigma_H + 0.25\sigma_V$ | 898.2 | 74.6 | 27.9 | 8.3 | 53.5 | 5.4 | -3.3 | 0.2 | -2.0 | -1.6 |
| $\sigma_A = 0.5\sigma_H + 0.5\sigma_V$ | 905.3 | 73.0 | 27.6 | 8.2 | 53.0 | 4.6 | -1.7 | 1.0 | -0.9 | -0.4 |
| $\sigma_A = 0.25\sigma_H + 0.75\sigma_V$ | 919.2 | 71.2 | 27.4 | 8.2 | 52.6 | 3.2 | -0.2 | 1.5 | 0.0 | 0.5 |

Note: The unit of the score is deaths. Lower scores and higher skill scores are better. Skill scores use vertical averaging from Table 1 as benchmark. Bold indicates the best method in each column.

Figure 13 Quantile skill scores averaged across all 52 Covid series for the 23 individual quantiles for the out-of-sample period for the averaging methods in (a), and weighted combining methods in (b). Higher values of the skill score are better.



5.7. Comparing Horizontal, Vertical and Angular Combining for Different Quantiles

Figure 13 reports quantile skill scores for the 23 probability levels for the methods in Table 1. The skill scores have been computed using the vertical average as the benchmark, and averaged across the out-of-sample period for all 52 series. In view of the results in Table 1 for horizontal averaging, it is not surprising to see that negative skill scores dominate Figure 13(a) for this method. However, the positive skill scores for this method for the extreme upper quantiles indicate that, for at least part of

the distributions, horizontal was more accurate than vertical averaging. It is interesting to compare the results for vertical and angular combining in Figures 13(a) and (b). Both plots show particularly strong results for angular combining in the tails of the distributions, while vertical combining was more competitive for the central quantiles. We can infer from this that for interval forecasts with a high nominal coverage probability, such as 95%, angular combining would be preferable for this dataset, while vertical and angular combining would both be reasonable choices for 50% intervals. In Online Appendix D.2, we provide plots showing the quantile skill scores separately for the U.S. national level series, and the high, medium and low mortality groupings of series.

We also evaluated accuracy across the 23 quantiles of each CDF forecast using unconditional calibration. We did this using reliability diagrams, which we present in Online Appendix D.3.

5.8. Evaluating Other Methods using the MQS

Although our aim in this paper is to introduce angular combining as an alternative to horizontal and vertical combining, it is also interesting to see how other methods from the literature perform for the mortality dataset. Table 3 reports the results for the methods listed below, along with the results from Table 1 for angular averaging and angular weighted combining, which we have positioned at the top of Table 3. Method parameters were optimized using the same approach that we employed to optimize θ for angular combining. For each series and forecast origin, this involved minimizing the in-sample MQS averaged over the four lead times.

Median aggregation – This is the simple method considered by Hora et al. (2013), which, as we showed in Section 4.5, produces the same CDF if implemented horizontally, vertically or at an angle.

Beta-transformed linear pool – Gneiting and Ranjan (2013) use the beta distribution to transform the CDF forecast of a vertical weighted combination. We implemented this with weights defined as in the weighted combinations of Table 1. The implementation involved optimizing the two parameters of the beta distribution.

Trimming – We implemented the trimming approach of Jose et al. (2014) that bases trimming on the mean of each CDF forecast. Exterior trimming involves averaging the CDF forecasts that remain after removing a percentage of the individual CDF forecasts with lowest and highest mean. Interior

trimming involves averaging the CDF forecasts that were among a percentage of those with lowest and highest mean. We implemented these methods with vertical, horizontal and angular averaging. Each form of trimming required the optimization of the trimming percentage.

Recalibration – Han and Budescu (2022) recalibrate a CDF forecast by transforming the probabilities corresponding to predefined bins. We applied the method to the three weighted combining methods in Table 1. We defined the bins as the 24 intervals bounded by the quantiles corresponding to the 23 probability levels of focus in the COVID-19 Forecast Hub, and the lower and upper bounds of each CDF. The method involved optimizing one parameter.

Table 3 For the Covid dataset, MQS for the out-of-sample period for a variety of combining and recalibration methods.

| | MQS | | | | | MQS skill score (%) | | | | |
|---|--------------|-------------|-------------|------------|-------------|---------------------|------------|------------|------------|------------|
| | U.S. | High | Medium | Low | All | U.S. | High | Medium | Low | All |
| <i>Angular combining (from Table 1)</i> | | | | | | | | | | |
| Angular averaging | 903.3 | 68.5 | 27.5 | 8.2 | 51.5 | 4.8 | 1.0 | 0.9 | 0.1 | 0.8 |
| Angular weighted combining | 839.1 | 66.6 | 27.2 | 8.1 | 49.4 | 11.6 | 4.0 | 2.4 | 1.1 | 2.7 |
| <i>Simple benchmark and transformed linear pool</i> | | | | | | | | | | |
| Median | 914.1 | 68.1 | 27.6 | 8.1 | 51.5 | 3.7 | 2.8 | 1.1 | 1.8 | 1.9 |
| Beta-transformed linear pool | 810.3 | 71.3 | 28.2 | 8.5 | 50.9 | 14.6 | 0.2 | -2.0 | -3.6 | -1.4 |
| <i>Exterior trimming</i> | | | | | | | | | | |
| Vertical | 896.4 | 67.0 | 27.3 | 8.1 | 50.7 | 5.6 | 4.3 | 1.8 | 2.1 | 2.8 |
| Horizontal | 897.0 | 79.3 | 27.8 | 8.2 | 55.0 | 5.5 | -4.8 | 0.4 | 0.5 | -1.2 |
| Angular | 901.0 | 68.6 | 27.6 | 8.1 | 51.4 | 5.1 | 2.0 | 1.0 | 1.2 | 1.5 |
| <i>Interior trimming</i> | | | | | | | | | | |
| Vertical | 951.0 | 72.3 | 27.7 | 8.2 | 53.7 | -0.2 | -2.0 | -0.3 | -0.3 | -0.9 |
| Horizontal | 897.4 | 98.0 | 28.8 | 8.5 | 61.5 | 5.4 | -14.4 | -3.5 | -6.0 | -7.6 |
| Angular | 905.3 | 97.6 | 27.8 | 8.3 | 61.1 | 4.6 | -11.0 | -0.3 | -1.1 | -3.9 |
| <i>Recalibration of weighted combining</i> | | | | | | | | | | |
| Vertical | 888.1 | 69.2 | 28.1 | 8.4 | 51.6 | 6.4 | -0.2 | -1.5 | -2.4 | -1.2 |
| Horizontal | 851.4 | 83.8 | 29.0 | 8.6 | 56.1 | 10.3 | -10.4 | -3.9 | -6.4 | -6.5 |
| Angular | 845.4 | 69.0 | 28.1 | 8.4 | 50.7 | 10.9 | 0.6 | -0.9 | -2.8 | -0.8 |

Note: The unit of the score is deaths. Lower scores and higher skill scores are better. Skill scores use vertical averaging from Table 1 as benchmark. Bold indicates the best method in each column.

In Table 3, angular weighted combining performs well, with the bold font indicating that it delivered the lowest MQS scores for four of the five categories. Turning to the other methods, we first note that the beta-transformed linear pool performed notably well for the U.S. national series, but apart from this, was uncompetitive with the better of the other methods. The best trimming method was exterior trimming with vertical averaging. In terms of the skill score averaged over all

52 series, this method was better than any other method, slightly outperforming angular weighted combining. Recalibration of the weighted combining methods did not lead to improvement in the results for these methods.

It could be suggested that angular combining can be approximated by a *secondary* weighted combination of the CDF forecasts produced by horizontal and vertical combining, with the weights related to the angle θ . When $\theta = 0^\circ$, the weight on the horizontal combination would equal 1, and when $\theta = 90^\circ$, the weight on the vertical combination would be 1. However, the question would then be whether to perform this secondary weighted combination horizontally or vertically. We implemented both possibilities, with the weights estimated by minimizing the sum of in-sample MQS. The third and fourth rows of values in Table 4 are the out-of-sample MQS results for horizontal and vertical secondary weighted combinations of the two CDF forecasts resulting from horizontal and vertical averaging of the individual CDF forecasts. The better of these two methods is not quite as accurate as angular averaging, which is included at the top of the table, and the poorer of the two methods is notably worse than angular averaging. In this comparison, angular averaging has the appeal of accuracy, and avoids the need to select between horizontal and vertical secondary weighted combining. Similar comments can be made when comparing the angular weighted combining results in the second row of the table, with the results in the bottom two rows, which correspond to secondary horizontal and vertical weighted combining of the two CDF forecasts produced by horizontal and vertical performance-weighted combining of the individual CDF forecasts.

Table 4 For the Covid dataset, MQS for the out-of-sample period for combinations of combinations, as well as angular combining.

| | MQS | | | | | MQS skill score (%) | | | | |
|--|--------------|-------------|-------------|------------|-------------|---------------------|------------|------------|------------|------------|
| | U.S. | High | Medium | Low | All | U.S. | High | Medium | Low | All |
| <i>Angular combining (from Table 1)</i> | | | | | | | | | | |
| Angular averaging | 903.3 | 68.5 | 27.5 | 8.2 | 51.5 | 4.8 | 1.0 | 0.9 | 0.1 | 0.8 |
| Angular weighted combining | 839.1 | 66.6 | 27.2 | 8.1 | 49.4 | 11.6 | 4.0 | 2.4 | 1.1 | 2.7 |
| <i>Combining horizontal & vertical averages</i> | | | | | | | | | | |
| Vertical secondary weighted combining | 914.0 | 76.3 | 28.1 | 8.2 | 54.4 | 3.7 | -6.3 | -1.4 | -0.3 | -2.5 |
| Horizontal secondary weighted combining | 901.9 | 69.9 | 27.7 | 8.2 | 51.9 | 5.0 | -1.3 | 0.3 | -0.4 | -0.4 |
| <i>Combining horizontal & vertical weighted combinations</i> | | | | | | | | | | |
| Vertical secondary weighted combining | 846.9 | 73.6 | 27.4 | 8.1 | 52.0 | 10.8 | -2.4 | 1.8 | 0.4 | 0.2 |
| Horizontal secondary weighted combining | 839.8 | 67.3 | 27.4 | 8.1 | 49.7 | 11.5 | 2.8 | 1.9 | 0.3 | 1.9 |

Note: The unit of the score is deaths. Lower scores and higher skill scores are better. Skill scores use vertical averaging from Table 1 as benchmark. Bold indicates the best method in each column.

6. Additional Empirical Studies

We now broaden our empirical analysis by considering data from surveys of professional economic forecasters in Section 6.1, and electricity price data in Section 6.2. The survey data is similar to the Covid dataset in the sense that the probabilistic forecasts are provided by a sizable number of experts using a wide variety of methods. By contrast, in our study of electricity prices, we combine a relatively small set of probabilistic forecasts, produced using several time series models. A further notable aspect of our analysis of electricity prices is that it involves a much longer dataset than our other two studies, enabling more accurate estimation of combining method parameters, and a clearer ranking of methods, supported by statistical testing to compare forecast accuracy.

6.1. Surveys of Professional Forecasters

Lichtendahl et al. (2013) compare horizontal and vertical averaging using probabilistic forecasts from the Survey of Professional Forecasters (SPF) of the Federal Reserve Bank of Philadelphia. Weighted combining is not considered for this data because there is not a sufficient record of historical accuracy for each forecaster. Each quarter, participants submit probabilistic forecasts of annual U.S. GDP growth and inflation. We follow Lichtendahl et al. (2013) in considering the forecasts made in each quarter for growth and inflation in the same calendar year. We use growth forecasts from the first quarter of 1982 to the fourth quarter of 2023, amounting to 168 quarters, and inflation forecasts from the fourth quarter of 1968 to the fourth quarter of 2023, which amounted to 221 quarters. For growth, the number of forecasters varied from 7 to 52, with a median of 32, and for inflation, it varied from 7 to 114, with a median of 34.

The U.S. SPF forecasts are also used by Jose et al. (2014) to evaluate their aggregation methods. In addition, they consider forecasts from the SPF of the European Central Bank (ECB). We do the same, and consider forecasts made in each quarter for GDP growth and inflation in the same calendar year, and also for unemployment, defined as the average of the monthly unemployment for the calendar year. Forecasts for the three variables were available from the first quarter of 1999 to the fourth quarter of 2023, which constituted 100 quarters. For growth, the number of forecasters had a median of 51, and varied between 40 and 65. It was similar for inflation and unemployment.

The probabilistic forecasts from both surveys are submitted in the form of a probability for each of a set of bins specified in the survey. To obtain a continuous CDF, like Lichtendahl et al. (2013) and Jose et al. (2014), we fitted piecewise-linear CDFs to the bin probabilities. As the number of periods in our SPF datasets were of a similar order of magnitude to our Covid dataset, for consistency, we used a similar length period for the initial in-sample estimation of combining method parameters, and then expanded the in-sample period as we stepped forward. With the focus being to forecast the economic variables for each calendar year, combining method parameters can only be re-estimated at the end of each year, as new observations only become available at that time. Allowing for this, and setting the initial estimation period to be at least 10 periods, led us to use an initial estimation period of 13 quarters for U.S. inflation, and 12 quarters for the other four series. In this way, an out-of-sample forecast was produced from $n-m$ forecast origins, where n and m are the numbers of quarters in the dataset and initial estimation period, respectively. We optimized parameters using the in-sample CRPS. For the actual observed growth, inflation and unemployment, we followed Clements (2018) in using the value for year T , released in the first quarter of year $T+1$.

Figure 14 shows the angle optimized at each forecast origin for each series. For U.S. growth, the angle did not vary greatly, starting at 90° and then remaining at about 75° for most of the forecast origins. For U.S. inflation, the fluctuations in the angle for the early forecast origins suggests that a larger sample size would have been better. After the initial instability, the angle steadily rose from 0° to about 50° . For ECB growth and inflation, the angle was 90° for almost all forecast origins, and for ECB unemployment, the angle was 0° or 90° for about three-quarters of the forecast origins.

Figure 14 For the SPF datasets and angular averaging, the optimized angle θ at each forecast origin for the five series.

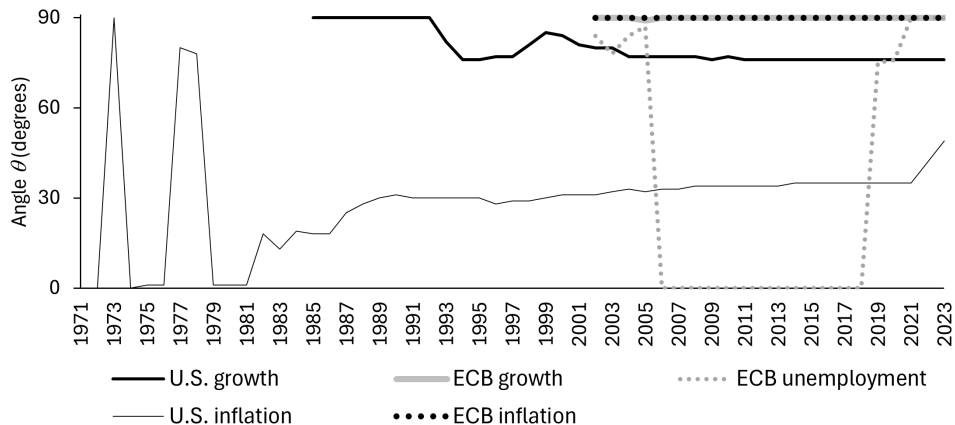


Table 5 presents the out-of-sample CRPS results for horizontal, vertical and angular averaging, along with switching between horizontal and vertical averaging. The table shows that angular averaging outperformed the other methods for the two U.S. series. In view of the optimized angles in Figure 14, it is understandable that the results for angular averaging were the same as vertical averaging for ECB growth and inflation. ECB unemployment was the only one of the five series for which angular averaging was outperformed. Online Appendix E.1 provides a comparison of methods in terms of the quantile skill scores for different quantile probability levels. These results show horizontal and angular averaging performing particularly well in the tails of the distributions. In Online Appendix E.2, the CRPS results for other methods show that the best results overall were obtained using exterior trimming with angular averaging.

Table 5 For the SPF datasets, CRPS for the out-of-sample period for the three forms of averaging and horizontal/vertical switching.

| | CRPS | | | | | | CRPS skill score (%) | | | | | |
|-------------------------------|-------------|-------------|-------------|-------------|-------------|-------------|----------------------|------------|------------|------------|------------|------------|
| | U.S. | | ECB | | ECB | | U.S. | | ECB | | ECB | |
| | Gro | Infl | Gro | Infl | Unem | All | Gro | Infl | Gro | Infl | Unem | All |
| Vertical averaging | 38.0 | 36.4 | 80.4 | 66.9 | 22.6 | 48.8 | 0.0 | 0.0 | 0.0 | 0.0 | 0.0 | 0.0 |
| Horizontal averaging | 38.1 | 35.9 | 81.4 | 67.9 | 23.2 | 49.3 | -0.2 | 1.4 | -1.3 | -1.6 | -2.9 | -0.9 |
| Horizontal/vertical switching | 38.0 | 36.1 | 80.4 | 66.9 | 22.6 | 48.8 | 0.0 | 0.9 | 0.0 | 0.0 | -0.2 | 0.2 |
| Angular averaging | 37.8 | 35.8 | 80.4 | 66.9 | 22.8 | 48.7 | 0.6 | 1.6 | 0.0 | 0.0 | -0.9 | 0.3 |

Note: Scores are percentages and have been multiplied by 100. Lower scores and higher skill scores are better. Skill scores use vertical averaging as benchmark. Bold indicates the best method in each column.

6.2. Electricity Prices

Our third empirical study uses hourly Nord Pool day-ahead electricity market clearing prices. The price for each hour is set the previous day, and this has led to models being fitted separately to the daily time series for each hour. We focused on day-ahead forecasting, and implemented the following methods for each of the 24 hourly time series:

Method 1. Historical simulation – As a simple benchmark, we used the piecewise-linear CDF constructed from the empirical distribution of the price for the same hour on the previous 28 days. Optimizing the number of previous days to use in the method led to fewer than 10, which we felt was unappealing as the basis for estimating a CDF, so we arbitrarily chose a period of one month.

Method 2. ARX – We fitted the following model considered by Nowotarski and Weron (2018),

$$p_{h,t} = \phi_{h,0} + \phi_{h,1}p_{h,t-1} + \phi_{h,2}p_{h,t-2} + \phi_{h,3}p_{h,t-7} + \phi_{h,4}mp_{t-1} + d_{h,1}D_{Mon,t} + d_{h,2}D_{Sat,t} + d_{h,3}D_{Sun,t} + \varepsilon_{h,t} \quad (8)$$

where $p_{h,t}$ is the log price for hour h on day t ; mp_t is the minimum value of the log price on day t ; $D_{Mon,t}$, $D_{Sat,t}$ and $D_{Sun,t}$ are binary variables indicating whether day t is a Monday, Saturday or Sunday, respectively; the $\phi_{h,i}$ and $d_{h,i}$ are parameters; and the $\varepsilon_{h,t}$ is an error term. We estimated the model using least squares. A CDF forecast was then constructed with the model's point forecast as the mean, and distribution around the mean obtained by applying the historical simulation approach to the last 28 residuals from the model, with the aim of capturing time-varying volatility.

Method 3. AR1-GARCH – This method has an AR(1) model for the mean of the log price, and the asymmetric GJR-GARCH(1,1) model for the variance. We estimated the model using maximum likelihood based on the skewed t distribution described by Christoffersen (2012, Chapter 6, Section 7). To construct each CDF forecast, we used the forecast of the mean and variance with distributional shape specified as the piecewise-linear CDF constructed from the empirical distribution of all standardized residuals.

Method 4. ARX-GARCH – This is identical to the AR1-GARCH method, except that the mean was modeled using (8). This model was fitted by Taylor (2021) to the same electricity price data.

Our dataset consisted of the 6×365 days starting on January 1 2013. Online Appendix F.1 presents the time series plot of the price for one hour of the day. As the time series were much longer than those in our other two empirical studies, we used a rolling window for estimation, which is more common than an expanding window when a reasonably long time series is available. An advantage of a rolling window is that it enables the straightforward application of Diebold-Mariano tests to compare forecast accuracy (Giacomini and White 2006). For each hour of our electricity price time series, we used a rolling window of 365 days for repeated re-estimation of the parameters in Methods 2 to 4. For all four methods, we produced out-of-sample day-ahead forecasts for the final 5×365 days. Using this period, we repeatedly re-estimated combining method parameters by minimizing the CRPS based on a rolling window of 365 days. This resulted in out-of-sample forecasts for the combining methods for the final 4×365 days. Given the availability of individual model forecasts

for the sizable in-sample period, we adapted the approach to computing combining weights that we used in our Covid study, so that the weight on each method was inversely proportional to the method’s CRPS raised to the power of a tuning parameter (see, for example, Stock and Watson 1999). This parameter was estimated for each weighted combining method at each forecast origin.

As the features of Methods 2 and 3 are captured by Method 4, it seemed likely this model would dominate weighted combinations. Therefore, we considered combinations involving three different selections of the four methods: Methods 1 and 2, Methods 1 to 3, and Methods 1 to 4.

For angular averaging of Methods 1 to 3, Figure 15 presents the histogram of the angles optimized at all 4×365 forecast origins for all 24 hourly series. Figure 16 shows the angle optimized at each forecast origin for the following four hourly series: midday, midnight, and the two hours in the day corresponding to the highest values of the median of the price for the entire sample of 6×365 days. Each series shows the angle steadily varying over time, fluctuating by about 30° between its minimum and maximum.

Figure 15 For the electricity price dataset and angular averaging of Methods 1 to 3, histogram of the angle θ optimized at each forecast origin for all 24 hourly series.

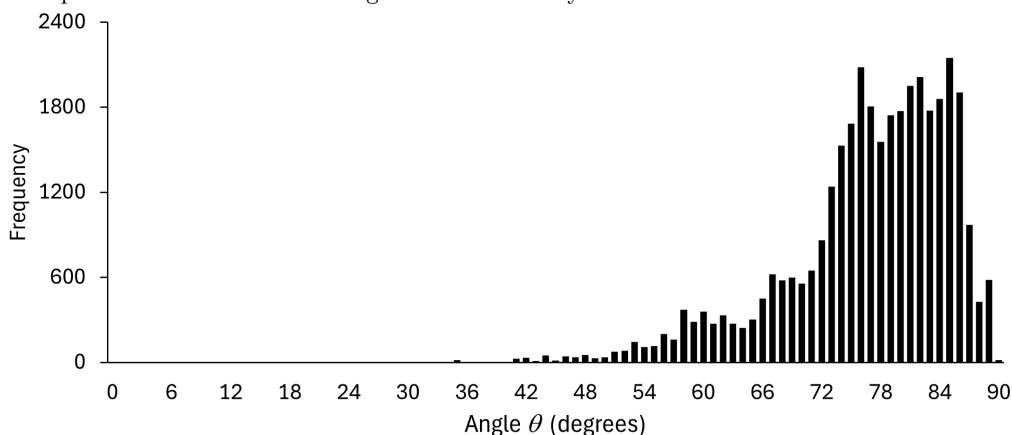


Figure 16 For the electricity price dataset and angular averaging of Methods 1 to 3, the optimized angle θ at each forecast origin for four of the hourly series.

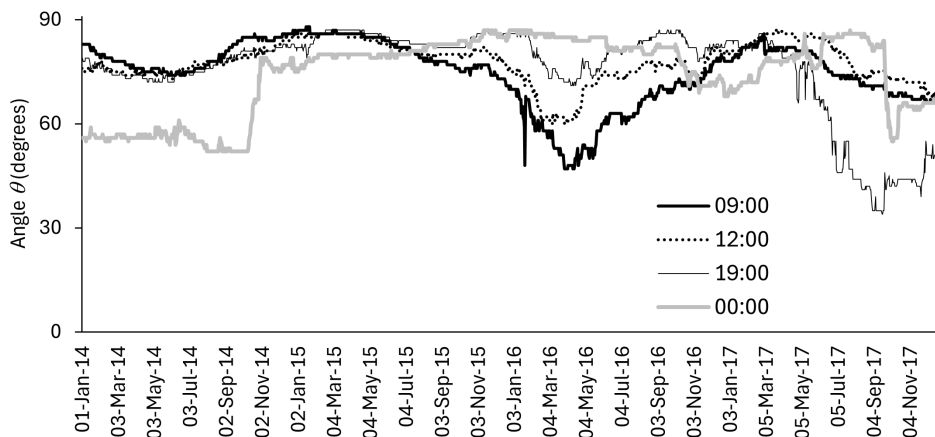


Table 6 shows the CRPS averaged across the out-of-sample period for all 24 hourly series for combining applied to the three selections of Methods 1 to 4. Comparing the methods involving averaging, horizontal averaging was the least accurate, the switching method performed similarly to vertical averaging, and angular averaging was the most accurate. We note that the angular average of Methods 1 to 3, and of Methods 1 to 4, was more accurate than the best of the four individual methods. The table shows weighted combining outperforming averaging. Of the weighted combining methods, angular combining performed the best. However, the difference between the best and worst weighted combining results was notably less than for the averaging methods.

Table 6 For the electricity price dataset, CRPS and CRPS skill score for the out-of-sample period of 4×365 days, averaged across all 24 hourly series for the four individual methods, combining methods, and horizontal/vertical switching applied to Methods 1 and 2, Methods 1 to 3, and Methods 1 to 4.

| | Methods 1 & 2 | | Methods 1 to 3 | | Methods 1 to 4 | |
|-------------------------------|---------------|-----------------|----------------|-----------------|----------------|-----------------|
| | CRPS | Skill score (%) | CRPS | Skill score (%) | CRPS | Skill score (%) |
| <i>Averaging</i> | | | | | | |
| Vertical | 187.1 | 0.0 | 178.9 | 0.0 | 173.1 | 0.0 |
| Horizontal | 191.6 | -2.6 | 181.1 | -1.4 | 174.9 | -1.2 |
| Horizontal/vertical switching | 187.3 | -0.1 | 178.9 | 0.0 | 173.1 | 0.0 |
| Angular | 186.0 | 0.6 | 177.7 | 0.6 | 172.2 | 0.4 |
| <i>Weighted combining</i> | | | | | | |
| Vertical | 176.4 | 6.1 | 171.9 | 3.9 | 169.8 | 1.9 |
| Horizontal | 177.9 | 5.3 | 171.4 | 4.1 | 170.0 | 1.8 |
| Horizontal/vertical switching | 176.5 | 6.0 | 171.5 | 4.1 | 169.8 | 1.9 |
| Angular | 175.6 | 6.5 | 170.7 | 4.5 | 169.4 | 2.1 |
| <i>Individual methods</i> | | | | | | |
| 1. Historical simulation | 267.1 | -43.6 | 267.1 | -51.5 | 267.1 | -56.7 |
| 2. ARX | 182.4 | 3.1 | 182.4 | -2.3 | 182.4 | -5.7 |
| 3. AR1-GARCH | NA | NA | 198.6 | -8.9 | 198.6 | -12.6 |
| 4. ARX-GARCH | NA | NA | NA | NA | 172.8 | 0.4 |

Note: Scores have unit EUR/MWh and have been multiplied by 100. Lower scores and higher skill scores are better. Skill scores use vertical averaging as benchmark. NA abbreviates “not applicable”. Bold indicates the best method in each column.

As this study involved a lengthy out-of-sample period, we performed statistical testing to compare the CRPS results. For combinations of Methods 1 to 3, Table 7 shows the number of hourly series, out of the 24, for which the Diebold-Mariano test indicated the CRPS for the method listed in the row was significantly lower than for the method listed in the column (using a 5% significance level). The row for angular averaging shows that it was significantly more accurate than the other averaging methods for more than half the 24 series. The column for the angular average shows that it was not significantly less accurate than the other averaging methods for any series. The row for

angular weighted combining shows that it was significantly more accurate than the other weighted combining methods for varying numbers of the 24 series, and significantly less accurate than none of them. Online Appendix F.2 shows similar results for combinations of Methods 1 and 2, and of Methods 1 to 4.

Table 7 For the electricity price dataset, Diebold-Mariano test results for combinations of Methods 1 to 3. Values are the number of hourly series, out of the 24, for which the CRPS for the method listed in the row was significantly lower than for the method listed in the column (using a 5% significance level).

| | <i>Averaging</i> | | | | | <i>Wtd combining</i> | | | | | <i>Indiv methods</i> | | | |
|-------------------------------|------------------|------------|-----------------|-----------|--|----------------------|------------|-----------------|---------|--|----------------------|-----------|--------------|--|
| | Vertical | Horizontal | Hor/vert switch | Angular | | Vertical | Horizontal | Hor/vert switch | Angular | | 1. Hist sim | 2. ARX | 3. AR1-GARCH | |
| <i>Averaging</i> | | | | | | | | | | | | | | |
| Vertical | NA | 7 | 0 | 0 | | 0 | 0 | 0 | 0 | | 24 | 5 | 16 | |
| Horizontal | 0 | NA | 0 | 0 | | 0 | 0 | 0 | 0 | | 24 | 2 | 14 | |
| Horizontal/vertical switching | 0 | 7 | NA | 0 | | 0 | 0 | 0 | 0 | | 24 | 5 | 16 | |
| Angular | 16 | 22 | 15 | NA | | 0 | 0 | 0 | 0 | | 24 | 6 | 16 | |
| <i>Weighted combining</i> | | | | | | | | | | | | | | |
| Vertical | 18 | 21 | 18 | 13 | | NA | 0 | 1 | 0 | | 24 | 24 | 23 | |
| Horizontal | 16 | 21 | 16 | 14 | | 2 | NA | 0 | 0 | | 24 | 24 | 23 | |
| Horizontal/vertical switching | 19 | 23 | 20 | 14 | | 2 | 0 | NA | 0 | | 24 | 24 | 23 | |
| Angular | 21 | 24 | 21 | 17 | | 15 | 4 | 12 | NA | | 24 | 24 | 23 | |
| <i>Individual methods</i> | | | | | | | | | | | | | | |
| 1. Historical simulation | 0 | 0 | 0 | 0 | | 0 | 0 | 0 | 0 | | NA | 0 | 0 | |
| 2. ARX | 0 | 2 | 0 | 0 | | 0 | 0 | 0 | 0 | | 24 | NA | 11 | |
| 3. AR1-GARCH | 0 | 1 | 0 | 0 | | 0 | 0 | 0 | 0 | | 24 | 4 | NA | |

Note: NA abbreviates "not applicable". Bold indicates the best method in each column.

In Online Appendix F.3, we present the CRPS for each hour of the day. Online Appendix F.4 provides the quantile skill scores for different quantile probability levels, and, as in the Covid and SPF studies, angular combining can be seen to perform particularly well in the tails of the distributions. Online Appendix F.5 evaluates other combining methods, and shows that the results for the beta-transformed linear pool matched those for angular weighted combining.

7. Summary and Concluding Remarks

In the literature on distributional forecasting, the question has been posed as to whether it is better to average horizontally or vertically. We have extended the debate by proposing combining at an angle, leading to a method that lies between the extremes of horizontal and vertical

combining. Although our proposal is motivated by empirical pragmatism, we also feel it is interesting conceptually. We extended the theoretical results of Lichtendahl et al. (2013) to obtain results for angular combining. Like vertical and horizontal combining, angular combining produces CDF forecasts for which the mean is the combination of the means of the individual CDF forecasts. Angular combining produces a CDF with lower variance than vertical combining, and, under certain assumptions, greater variance than horizontal combining. As with vertical and horizontal averaging, the CRPS for angular averaging is no worse than the average CRPS of the individual CDF forecasts. In Online Appendix G, we present a new modeling framework that reveals how horizontal, vertical and angular combining structure the available information differently, providing insight for when it is most natural to use each combining method, and showing potential for new approaches to combining.

In our empirical studies, angular combining performed well in comparison with horizontal and vertical combining, with noticeably strong performance in terms of the accuracy of the tails of the distributions. It was also found to be competitive when compared against a variety of combining and recalibration methods from the literature. We included an angular combining version of the trimming-based method of Jose et al. (2014), demonstrating that angular combining should not be viewed as a single method because it allows a different approach to existing combining methods.

References

- Aastveit, K. A., Mitchell, J., Ravazzolo, F., and van Dijk, H. K. (2019). The evolution of forecast density combinations in economics. In *Oxford Research Encyclopedia of Economics and Finance*.
- Adam, D. (2020). Special report: The simulations driving the world's response to covid-19. *Nature*, 580(7802):316–319.
- Arrow, K. J., Harris, T., and Marschak, J. (1951). Optimal inventory policy. *Econometrica: Journal of the Econometric Society*, pages 250–272.
- Bamber, J., Aspinall, W., and Cooke, R. (2016). A commentary on "how to interpret expert judgment assessments of twenty-first century sea-level rise" by Hylke de Vries and Roderik SW van de Wal. *Climatic Change*, 137(3):321–328.
- Bracher, J., Ray, E. L., Gneiting, T., and Reich, N. G. (2021). Evaluating epidemic forecasts in an interval format. *PLOS Computational Biology*, 17(2):e1008618.
- Brownlees, C. and Souza, A. B. (2021). Backtesting global growth-at-risk. *Journal of Monetary Economics*, 118:312–330.
- Busetti, F. (2017). Quantile aggregation of density forecasts. *Oxford Bulletin of Economics and Statistics*, 79(4):495–512.
- Chernozhukov, V., Fernández-Val, I., and Galichon, A. (2010). Quantile and probability curves without crossing. *Econometrica*, 78(3):1093–1125.

- Christoffersen, P. F. (2012). *Elements of Financial Risk Management (2nd ed.)*. Waltham: Academic Press.
- Clements, M. P. (2018). Are macroeconomic density forecasts informative? *International Journal of Forecasting*, 34(2):181–198.
- Colson, A. R. and Cooke, R. M. (2017). Cross validation for the classical model of structured expert judgment. *Reliability Engineering & System Safety*, 163:109–120.
- Cooke, R. M. (2022). Averaging quantiles, variance shrinkage, and overconfidence. *Futures & Foresight Science*, page e139.
- Cooke, R. M., Marti, D., and Mazzuchi, T. (2021). Expert forecasting with and without uncertainty quantification and weighting: What do the data say? *International Journal of Forecasting*, 37(1):378–387.
- Fakoor, R., Kim, T., Mueller, J., Smola, A. J., and Tibshirani, R. J. (2023). Flexible model aggregation for quantile regression. *Journal of Machine Learning Research*, 24:162–1.
- Giacomini, R. and White, H. (2006). Tests of conditional predictive ability. *Econometrica*, 74(6):1545–1578.
- Gneiting, T. and Raftery, A. E. (2007). Strictly proper scoring rules, prediction, and estimation. *Journal of the American Statistical Association*, 102(477):359–378.
- Gneiting, T. and Ranjan, R. (2013). Combining predictive distributions. *Electronic Journal of Statistics*, 7:1747–1782.
- Grushka-Cockayne, Y., Jose, V. R. R., and Lichtendahl, K. C. (2017a). Ensembles of overfit and overconfident forecasts. *Management Science*, 63(4):1110–1130.
- Grushka-Cockayne, Y., Lichtendahl, K. C., Jose, V. R. R., and Winkler, R. L. (2017b). Quantile evaluation, sensitivity to bracketing, and sharing business payoffs. *Operations Research*, 65(3):712–728.
- Hall, S. G. and Mitchell, J. (2007). Combining density forecasts. *International Journal of Forecasting*, 23(1):1–13.
- Han, Y. and Budescu, D. V. (2022). Recalibrating probabilistic forecasts to improve their accuracy. *Judgment and Decision Making*, 17(1):91–123.
- Hora, S. C. (2004). Probability judgments for continuous quantities: Linear combinations and calibration. *Management Science*, 50(5):597–604.
- Hora, S. C., Fransen, B. R., Hawkins, N., and Susel, I. (2013). Median aggregation of distribution functions. *Decision Analysis*, 10(4):279–291.
- Jose, V. R. R., Grushka-Cockayne, Y., and Lichtendahl, K. C. (2014). Trimmed opinion pools and the crowd’s calibration problem. *Management Science*, 60(2):463–475.
- Jose, V. R. R. and Winkler, R. L. (2009). Evaluating quantile assessments. *Operations Research*, 57(5):1287–1297.
- Kapetanios, G., Mitchell, J., Price, S., and Fawcett, N. (2015). Generalised density forecast combinations. *Journal of Econometrics*, 188(1):150–165.
- Knüppel, M. and Krüger, F. (2022). Forecast uncertainty, disagreement, and the linear pool. *Journal of Applied Econometrics*, 37(1):23–41.
- Larrick, R. P., Mannes, A. E., and Soll, J. B. (2012). The social psychology of the wisdom of crowds. In *Social Judgment and Decision Making*, pages 227–242. Psychology Press.
- Lichtendahl, K. C., Grushka-Cockayne, Y., and Winkler, R. L. (2013). Is it better to average probabilities or quantiles? *Management Science*, 59(7):1594–1611.
- Makridakis, S., Spiliotis, E., Assimakopoulos, V., Chen, Z., Gaba, A., Tsetlin, I., and Winkler, R. L. (2022). The M5 uncertainty competition: Results, findings and conclusions. *International Journal of Forecasting*, 38(4):1365–1385.
- Marcjasz, G., Uniejewski, B., and Weron, R. (2020). Probabilistic electricity price forecasting with narx networks: Combine point or probabilistic forecasts? *International Journal of Forecasting*, 36(2):466–479.
- Moore, D. A. and Healy, P. J. (2008). The trouble with overconfidence. *Psychological Review*, 115(2):502.
- Nowotarski, J. and Weron, R. (2018). Recent advances in electricity price forecasting: A review of probabilistic forecasting. *Renewable and Sustainable Energy Reviews*, 81:1548–1568.

-
- Raftery, A. E., Gneiting, T., Balabdaoui, F., and Polakowski, M. (2005). Using bayesian model averaging to calibrate forecast ensembles. *Monthly Weather Review*, 133(5):1155–1174.
- Ray, E. L., Brooks, L. C., Bien, J., Biggerstaff, M., Bosse, N. I., Bracher, J., Cramer, E. Y., Funk, S., Gerding, A., Johansson, M. A., et al. (2023). Comparing trained and untrained probabilistic ensemble forecasts of covid-19 cases and deaths in the united states. *International journal of forecasting*, 39(3):1366–1383.
- Soll, J. B., Palley, A. B., Klayman, J., and Moore, D. A. (2023). Overconfidence in probability distributions: People know they don’t know, but they don’t know what to do about it. *Management Science*. Forthcoming.
- Stock, J. and Watson, M. (1999). *A Comparison of Linear and Nonlinear Univariate Models for Forecasting Macroeconomic Time Series*, pages 1–44. Oxford University Press, Oxford.
- Stone, M. (1961). The opinion pool. *The Annals of Mathematical Statistics*, pages 1339–1342.
- Surowiecki, J. (2004). *The wisdom of crowds: Why the many are smarter than the few*. Number 5. New York: Doubleday.
- Taylor, J. W. (2021). Evaluating quantile-bounded and expectile-bounded interval forecasts. *International Journal of Forecasting*, 37(2):800–811.
- Taylor, J. W. and Jeon, J. (2018). Probabilistic forecasting of wave height for offshore wind turbine maintenance. *European Journal of Operational Research*, 267(3):877–890.
- Taylor, J. W. and Taylor, K. S. (2023). Combining probabilistic forecasts of covid-19 mortality in the united states. *European Journal of Operational Research*, 304(1):25–41.
- Taylor, K. S. and Taylor, J. W. (2022). Interval forecasts of weekly incident and cumulative covid-19 mortality in the united states: A comparison of combining methods. *PLOS One*, 17(3):e0266096.
- Thomas, E. A. and Ross, B. H. (1980). On appropriate procedures for combining probability distributions within the same family. *Journal of Mathematical Psychology*, 21(2):136–152.
- Uniejewski, B., Marcjasz, G., and Weron, R. (2019). On the importance of the long-term seasonal component in day-ahead electricity price forecasting: Part II - probabilistic forecasting. *Energy Economics*, 79:171–182.
- Uniejewski, B. and Weron, R. (2021). Regularized quantile regression averaging for probabilistic electricity price forecasting. *Energy Economics*, 95:105121.
- van der Meer, D., Pinson, P., Camal, S., and Kariniotakis, G. (2024). Crps-based online learning for nonlinear probabilistic forecast combination. *International Journal of Forecasting*.
- Wang, R. and Zitikis, R. (2021). An axiomatic foundation for the expected shortfall. *Management Science*, 67(3):1413–1429.
- Winkler, R. L., Grushka-Cockayne, Y., Lichtendahl, K. C., and Jose, V. R. R. (2019). Probability forecasts and their combination: A research perspective. *Decision Analysis*, 16(4):239–260.
- Ye, H., Luedtke, J., and Shen, H. (2019). Call center arrivals: When to jointly forecast multiple streams? *Production and Operations Management*, 28(1):27–42.